Open access • Posted Content • DOI:10.1101/2021.06.01.446579

SARS-CoV-2 Spreads through Cell-to-Cell Transmission — Source link

Cong Zeng, John P. Evans, Tiffany King, Tiffany King ...+6 more authors

Institutions: Ohio State University, Nationwide Children's Hospital, Washington University in St. Louis, Ohio Agricultural Research and Development Center

Published on: 01 Jun 2021 - bioRxiv (Cold Spring Harbor Laboratory)

Topics: Coronavirus, Infectivity and Neutralizing antibody

Related papers:

- Different Neutralization Sensitivity of SARS-CoV-2 Cell-to-Cell and Cell-Free Modes of Infection to Convalescent Sera.
- Systematic analysis of SARS-CoV-2 infection of an ACE2-negative human airway cell.
- Antibody-dependent SARS coronavirus infection is mediated by antibodies against spike proteins
- Inhibition of Coronavirus Entry In Vitro and Ex Vivo by a Lipid-Conjugated Peptide Derived from the SARS-CoV-2 Spike Glycoprotein HRC Domain.
- mRNA induced expression of human angiotensin-converting enzyme 2 in mice for the study of the adaptive immune response to severe acute respiratory syndrome coronavirus 2.

Share this paper:

View more about this paper here: https://typeset.io/papers/sars-cov-2-spreads-through-cell-to-cell-transmission-3w49t7tgmt

bioRxiv preprint doi: https://doi.org/10.1101/2021.06.01.446579; this version posted June 1, 2021. The copyright holder for this preprint (which was not certified by peer review) is the author/funder, who has granted bioRxiv a license to display the preprint in perpetuity. It is made available under aCC-BY-NC 4.0 International license.

1 **SARS-CoV-2 Spreads through Cell-to-Cell Transmission**
2
3
4 Cong Zeng[1,2], John P. Evans[1,2,3], Tiffany King[4,5], Yi-Min Zheng[1,2], Eugene M.
5 Oltz[6], Sean P. J. Whelan[7], Linda Saif [8, 9,10], Mark E. Peeples[4,5,10],
6 and Shan-Lu Liu[1,2,6, 10 *]
7
8 [1] Center for Retrovirus Research, The Ohio State University, Columbus,
9 OH 43210, USA
10 [2] Department of Veterinary Biosciences, The Ohio State University,
11 Columbus, OH 43210, USA
12 [3] Molecular, Cellular and Developmental Biology Program, The Ohio State
13 University, Columbus, OH 43210, USA
14 [4] Center for Vaccines & Immunity, Abigail Wexner Research Institute,
15 Nationwide Children's Hospital, Columbus, OH 43205, USA
16 [5] Department of Pediatrics, The Ohio State University College of Medicine,
17 Columbus, OH 43205, USA
18 [6] Department of Microbial Infection and Immunity, The Ohio State University
19 College of Medicine, Columbus, OH 43210, USA
20 [7] Department of Molecular Microbiology, Washington University School of
21 Medicine, St. Louis, MO 63110, USA
22 [8] Center for Food Animal Health, Animal Sciences Department, OARDC, College
23 of Food, Agricultural and Environmental Sciences, Wooster, OH 44691, USA
24 [9] Veterinary Preventive Medicine Department, College of Veterinary Medicine,
25 The Ohio State University, Wooster, OH 44691, USA
26 [10] Viruses and Emerging Pathogens Program, Infectious Diseases
27 Institute, The Ohio State University, Columbus, OH 43210, USA
28
29
30 * To whom correspondence should be addressed: Dr. Shan-Lu Liu
31 The Ohio State University, Columbus, OH 43210, USA,
32 Tel: (614) 292-8690; Email: liu.6244@osu.edu
33
34
35 **Key words:** SARS-CoV-2; cell-to-cell transmission; cell-cell fusion;
36 neutralization; variants of concern

bioRxiv preprint doi: https://doi.org/10.1101/2021.06.01.446579; this version posted June 1, 2021. The copyright holder for this preprint (which was not certified by peer review) is the author/funder, who has granted bioRxiv a license to display the preprint in perpetuity. It is made available under aCC-BY-NC 4.0 International license.

37 **ABSTRACT**
38
39 Severe acute respiratory syndrome coronavirus 2 (SARS-CoV-2) is a highly
40 transmissible coronavirus responsible for the global COVID-19 pandemic. Herein
41 we provide evidence that SARS-CoV-2 spreads through cell-cell contact in cultures,
42 mediated by the spike glycoprotein. SARS-CoV-2 spike is more efficient in
43 facilitating cell-to-cell transmission than SARS-CoV spike, which reflects, in part,
44 their differential cell-cell fusion activity. Interestingly, treatment of cocultured cells
45 with endosomal entry inhibitors impairs cell-to-cell transmission, implicating
46 endosomal membrane fusion as an underlying mechanism. Compared with cell-
47 free infection, cell-to-cell transmission of SARS-CoV-2 is refractory to inhibition by
48 neutralizing antibody or convalescent sera of COVID-19 patients. While ACE2
49 enhances cell-to-cell transmission, we find that it is not absolutely required.
50 Notably, despite differences in cell-free infectivity, the variants of concern (VOC)
51 B.1.1.7 and B.1.351 have similar cell-to-cell transmission capability. Moreover,
52 B.1.351 is more resistant to neutralization by vaccinee sera in cell-free infection,
53 whereas B.1.1.7 is more resistant to inhibition by vaccine sera in cell-to-cell
54 transmission. Overall, our study reveals critical features of SARS-CoV-2 spike-
55 mediated cell-to-cell transmission, with important implications for a better
56 understanding of SARS-CoV-2 spread and pathogenesis.
57

bioRxiv preprint doi: https://doi.org/10.1101/2021.06.01.446579; this version posted June 1, 2021. The copyright holder for this preprint (which was not certified by peer review) is the author/funder, who has granted bioRxiv a license to display the preprint in perpetuity. It is made available under aCC-BY-NC 4.0 International license.

58 **INTRODUCTION**

59 SARS-CoV-2 is a novel beta-coronavirus that is closely related to two other
60 pathogenic human coronaviruses, SARS-CoV and MERS-CoV (Chan et al., 2020).
61 The spike (S) proteins of SARS-CoV-2 and SARS-CoV mediate entry into target
62 cells, and both use angiotensin-converting enzyme 2 (ACE2) as the primary
63 receptor (Huang et al., 2020; Lan et al., 2020; Li, 2016; Walls et al., 2020; Zhou et
64 al., 2020b). The spike protein of SARS-CoV-2 is also responsible for induction of
65 neutralizing antibodies, thus playing a critical role in host immunity to viral infection
66 (Barnes et al., 2020; Baum et al., 2020; Rogers et al., 2020; Zost et al., 2020).

67 Similar to HIV and other class I viral fusion proteins, SARS-CoV-2 spike is
68 synthesized as a precursor that is subsequently cleaved and highly glycosylated;
69 these properties are critical for regulating viral fusion activation, native spike
70 structure and evasion of host immunity (Duan et al., 2020; Stewart-Jones et al.,
71 2016; Sun et al., 2020; Watanabe et al., 2020; White et al., 2008). However, distinct
72 from SARS-CoV, yet similar to MERS-CoV, the spike protein of SARS-CoV-2 is
73 cleaved by furin into S1 and S2 subunits during the maturation process in producer
74 cells (Chu et al., 2021; Coutard et al., 2020; Walls et al., 2020). S1 is responsible
75 for binding to the ACE2 receptor, whereas S2 mediates viral membrane fusion
76 (Shang et al., 2020; Wang et al., 2020). SARS-CoV-2 spike can also be cleaved
77 by additional host proteases, including transmembrane serine protease 2
78 (TMPRSS2) on the plasma membrane and several cathepsins in the endosome,

bioRxiv preprint doi: https://doi.org/10.1101/2021.06.01.446579; this version posted June 1, 2021. The copyright holder for this preprint (which was not certified by peer review) is the author/funder, who has granted bioRxiv a license to display the preprint in perpetuity. It is made available under aCC-BY-NC 4.0 International license.

79 which facilitate viral membrane fusion and entry into host cells (Brooke and Prischi,
80 2020; Hoffmann et al., 2020; Lukassen et al., 2020).

81 Enveloped viruses spread in cultured cells and tissues via two routes: by cell-
82 free particles and through cell-cell contact (Dale et al., 2011; Law et al., 2016;
83 Mothes et al., 2010; Sattentau, 2008). The latter mode of viral transmission
84 normally involves tight cell-cell contacts, sometimes forming virological synapses,
85 where local viral particle density increases (Zhong et al., 2013b), resulting in
86 efficient transfer of virus to neighboring cells (Mothes et al., 2010). Additionally,
87 cell-to-cell transmission has the ability to evade antibody neutralization, accounting
88 for efficient virus spread and pathogenesis, as has been shown for HIV and HCV
89 (Brimacombe et al., 2011; Dale et al., 2013; Li et al., 2017; Miao et al., 2016; Zhong
90 et al., 2013a). Low levels of neutralizing antibodies, as well as a deficiency in type
91 I IFNs, have been reported for SARS-CoV-2 (Acharya et al., 2020; Jeyanathan et
92 al., 2020; Lowery et al., 2021; Shang et al., 2020; Zhang et al., 2020b; Zhou et al.,
93 2020a), and may have contributed to the COVID-19 pandemic and disease
94 progression (Carvalho et al., 2021; Chu et al., 2020; Dispinseri et al., 2021; Hui et
95 al., 2020; Park and Iwasaki, 2020; Yang et al., 2020).

96 In this work, we evaluated cell-to-cell transmission of SARS-CoV-2 in the
97 context of cell-free infection and in comparison to SARS-CoV. Results from this in
98 vitro study reveal the heretofore unrecognized role of cell-to-cell transmission that

bioRxiv preprint doi: https://doi.org/10.1101/2021.06.01.446579; this version posted June 1, 2021. The copyright holder for this preprint (which was not certified by peer review) is the author/funder, who has granted bioRxiv a license to display the preprint in perpetuity. It is made available under aCC-BY-NC 4.0 International license.

99 potentially impacts SARS-CoV-2 spread, pathogenesis and shielding from
100 antibodies in vivo.
101

102 RESULTS

103 **The spike protein of SARS-CoV-2 efficiently mediates cell-to-cell**
104 **transmission of lentiviral pseudotypes**. The spike is the only viral
105 transmembrane protein that directly mediates SARS-CoV-2 entry into host cells.
106 We evaluated if the spike protein of SARS-CoV-2 is critical for viral spread through
107 cell-cell contact. In order to compare the efficiency of cell-to-cell vs. cell-free
108 infection mediated by the spike proteins of SARS-CoV-2 and SARS-CoV, we took
109 advantage of an intron-gaussia luciferase (inGluc) HIV-1 lentiviral vector bearing
110 the spike of interest. In this system, the cells producing the inGluc lentiviral virions
111 bearing the spike protein cannot themselves express Gluc because the intron is
112 only removed during splicing of the virion genome transcribed from the integrated
113 genome and not during the production of Gluc mRNA. However, when that
114 lentivirus pseudotype enters a target cell, that genome is reverse transcribed and
115 integrated in a new cell, and the CMV promotor drives transcription of the now
116 intron-less Gluc transcript leading to Gluc protein production (Agosto et al., 2014;
117 Mazurov et al., 2010). We measured Gluc activity as a readout to compare the cell-
118 to-cell and cell-free infection efficiencies (**Figure 1A and Figure 1B**; see Methods).
119 Because cell-contact-mediated infection comprises both cell-to-cell transmission

bioRxiv preprint doi: https://doi.org/10.1101/2021.06.01.446579; this version posted June 1, 2021. The copyright holder for this preprint (which was not certified by peer review) is the author/funder, who has granted bioRxiv a license to display the preprint in perpetuity. It is made available under aCC-BY-NC 4.0 International license.

120 and cell-free infection, we calculated the efficiency of cell-to-cell transmission by
121 subtracting the portion of cell-free infection performed in parallel (see Methods).
122 Despite a relatively low level of SARS-CoV-2 cell-to-cell transmission
123 compared to SARS-CoV after 48 hr when coculturing of spike-bearing inGluc
124 lentiviral pseudotype producer cells and 293T cells stably expressing human ACE2
125 (293T/ACE2), we observed similar levels of cell-to-cell transmission between
126 SARS-CoV-2 and SARS-CoV by 72 hr, indicating a more efficient spread of SARS-
127 CoV-2 (**Figure 1C**). In contrast, the rate of cell-free infection of SARS-CoV was
128 much higher than that of SARS-CoV-2, i.e., approximately 10-fold, as measured
129 at 48 and 72 hr post-infection (**Figure 1D**). Flow cytometric analysis of viral
130 producer cells showed that the expression of SARS-CoV spike was higher than
131 that of SARS-CoV-2 (**Figure 1E**), in agreement with our previous report (Zeng et
132 al., 2020). By averaging results from six independent experiments, we estimated
133 that cell-to-cell transmission contributed to >90% of the total SARS-CoV-2 spread
134 in the coculturing system, as compared to ~60% for SARS-CoV performed in
135 identical experimental settings (**Figure 1F**). Parallel experiments were also
136 performed by using a *Transwell* system, which showed ~90% cell-to-cell vs. ~10%
137 cell-free infection for SARS-CoV-2 compared with ~77% cell-to-cell vs. ~23% cell-
138 free for SARS-CoV (**Figure 1G**). Collectively, these results revealed that the spike
139 protein of SARS-CoV-2 mediates cell-to-cell transmission more efficiently than the

bioRxiv preprint doi: https://doi.org/10.1101/2021.06.01.446579; this version posted June 1, 2021. The copyright holder for this preprint (which was not certified by peer review) is the author/funder, who has granted bioRxiv a license to display the preprint in perpetuity. It is made available under aCC-BY-NC 4.0 International license.

140 spike protein of SARS-CoV. However, the SARS-CoV spike is more capable of
141 mediating cell-free infection compared with SARS-CoV-2.
142
143 **Recombinant VSV (rVSV) expressing SARS-CoV-2 spike spreads faster than**
144 **rVSV bearing SARS-CoV spike.** We next compared the spreading infection of
145 replication-competent rVSV expressing SARS-CoV-2 or SARS-CoV spike. This
146 system has been previously used to study the cell-cell transmission of Ebolavirus
147 (EBOV) mediated by the glycoprotein, GP (Miao et al., 2016). Vero cells were
148 inoculated with a relatively low MOI (0.01) of rVSV expressing GFP and SARS-
149 CoV-2 spike in the place of VSV G protein (rVSV-GFP-SARS-CoV-2) or SARS-
150 CoV spike (rVSV-GFP-SARS-CoV) (Case et al., 2020). Cells were overlayed by
151 1% methylcellulose to block viral diffusion, and the number and size of GFP-
152 positive plaques were stained and determined by fluorescence microscopy.
153 Despite similar numbers of GFP-positive plaques between SARS-CoV-2 and
154 SARS-CoV, which confirmed equivalent inoculations, the sizes for SARS-CoV-2
155 plaques were noticeably larger, as inspected at 18 and 24 hr post-infection (**Figure**
156 **2A and Figure 2B**). Quantitative analyses of data at 72 hr showed that the size of
157 SARS-CoV-2 plaques (diameter (0.93 ± 0.03) mm) was about 2 times greater than
158 that of SARS-CoV (diameter (0.53 ± 0.02) mm), whereas the plaque numbers
159 between SARS-CoV-2 and SARS-CoV were comparable (**Figure 2C and Figure**
160 **2D**).

bioRxiv preprint doi: https://doi.org/10.1101/2021.06.01.446579; this version posted June 1, 2021. The copyright holder for this preprint (which was not certified by peer review) is the author/funder, who has granted bioRxiv a license to display the preprint in perpetuity. It is made available under aCC-BY-NC 4.0 International license.

161 We next attempted to visualize cell-to-cell transmission of rVSV-GFP-SARS-
162 CoV-2 by imaging fluorescent dye transfer in cocultured cells, either in the
163 presence of methylcellulose or monoclonal antibody 2B04 against the SARS-CoV-
164 2 spike. In this experiment, donor Vero cells were infected with rVSV-GFP-SARS-
165 CoV-2 at different MOIs and subsequently cocultured with target Vero cells stably
166 expressing mTomato (Vero-mTomato-Red). Efficient transmission was detected
167 using fluorescence microscopy, as well as by flow cytometry at 6 h, with 23.9%
168 double positive cell populations (**Figure S1A and Figure S1B**). Treating
169 cocultured cells with methylcellulose, which has been found to prevent cell-free
170 infection by drastically by reducing the diffusion of virions between cells (Mothes
171 et al., 2010), or 2B04 that potently inhibit cell-free infection (Zeng et al., 2020),
172 reduced the cell-to-cell transmission to 12.7% and 5.38%, respectively. Combining
173 results from multiple independent experiments, we estimated that ~50% of the total
174 infection came from cell-to-cell transmission, which was still partially blocked by
175 2B04 (**Figure S1C**). Similar experiments performed in parallel for rVSV-GFP-
176 SARS-CoV showed a stronger inhibition by methylcellulose (~65%), suggesting a
177 more efficient cell-free infection of rVSV-GFP-SARS-CoV compared with that of
178 SARS-CoV-2. Importantly, 2B04 had no effect on cell-to-cell or cell-free infection
179 of rVSV-GFP-SARS-CoV as would be expected since 2B04 does not cross-react
180 with SARS-CoV (**Figures S1D-S1F**) (Alsoussi et al., 2020; Zeng et al., 2020).
181 Altogether, these results demonstrated that, similar to lentiviral pseudotypes, the

bioRxiv preprint doi: https://doi.org/10.1101/2021.06.01.446579; this version posted June 1, 2021. The copyright holder for this preprint (which was not certified by peer review) is the author/funder, who has granted bioRxiv a license to display the preprint in perpetuity. It is made available under aCC-BY-NC 4.0 International license.

182 spike protein of SARS-CoV-2 more efficiently mediates the cell-to-cell
183 transmission of rVSV-GFP than SARS-CoV.
184
185 **The higher cell-cell fusion activity of SARS-CoV-2 spike contributes to**
186 **efficient cell-to-cell transmission.** We next explored if cell-cell fusion by SARS-
187 CoV-2 spike plays a role in cell-to-cell transmission. To this end, we co-transfected
188 293T cells with plasmids expressing the inGluc lentiviral vector, SARS-CoV-2 or
189 SARS-CoV spike, and GFP. The transfected producer cells were cocultured with
190 target 293T/ACE2 cells; syncytia formation and cell-to-cell transmission were
191 measured over time. Following ~2 h of coculturing, we observed small but apparent
192 syncytia for SARS-CoV-2, yet with no syncytia formation for SARS-CoV (**Figure**
193 **3A**). At 24 h following coculturing, more syncytia formation, with larger sizes, was
194 observed in cells expressing SARS-CoV-2 spike, whereas fewer and smaller
195 syncytia were seen for SARS-CoV (**Figure 3A**). The difference between SARS-
196 CoV-2 and SARS-CoV spike-induced cell-cell fusion was further evaluated by a
197 more quantitative, Tet-off-based fusion assay, which showed a ~5-fold higher
198 fusion activity of SARS-CoV-2 compared with that of SARS-CoV (**Figure 3B**).
199 We next treated cocultured cells with a pan-coronavirus fusion peptide inhibitor
200 EK1 that has been shown to inhibit fusion of SARS-CoV-2, SARS-CoV, and other
201 related CoVs (Xia et al., 2019; Xia et al., 2020), and simultaneously measured its
202 effect on cell-cell fusion and cell-to-cell transmission. Syncytia formation of SARS-

bioRxiv preprint doi: https://doi.org/10.1101/2021.06.01.446579; this version posted June 1, 2021. The copyright holder for this preprint (which was not certified by peer review) is the author/funder, who has granted bioRxiv a license to display the preprint in perpetuity. It is made available under aCC-BY-NC 4.0 International license.

203 CoV-2 was strongly inhibited by EK1 (**Figure 3C**), in accordance with its effect on
204 cell-to-cell transmission (**Figure 3D**). Unexpectedly, although EK1 inhibited the
205 ability of SARS-CoV spike to induce small syncytia, we did not find obvious
206 inhibition of EK1 on SARS-CoV spike-mediated cell-to-cell transmission (**Figure**
207 **3C and Figure 3D)**. To investigate if these results were cell-type dependent, we
208 performed similar experiments using human intestine epithelial Caco-2 as target
209 cells and found that EK1 indeed inhibited the cell-to-cell transmission of both
210 SARS-CoV-2 and SARS-CoV (**Figure 3E**). Overall, these results support the
211 notion that the strong cell-cell fusion activity of SARS-CoV-2 spike contributes, but
212 may not solely determine, its efficient cell-to-cell transmission.
213
214 **ACE2 enhances but is not required for cell-to-cell transmission.** ACE2 is the
215 primary receptor of both SARS-CoV-2 and SARS-CoV, mediating viral entry into
216 host cells. We next evaluated the role of ACE2 in cell-to-cell transmission as
217 compared with cell-free infection. We observed increased cell-to-cell and cell-free
218 infection when more plasmid encoding ACE2 was transfected into the target 293T
219 cells, as would be expected (**Figure 4A** and **Figure 4B**). Interestingly, with a
220 relatively low dose of ACE2 (i.e., 0.2 μg), SARS-CoV-2 reached ~70% of its
221 maximal cell-to-cell transmission (at 0.5 μg ACE2). In contrast, SARS-CoV showed
222 ~30% maximal cell-to-cell transmission at 1.5 μg ACE2 (**Figure 4A and Figure**
223 **4B**). Notably, when the highest dose of ACE2 (1.5 μg) was transfected into target

bioRxiv preprint doi: https://doi.org/10.1101/2021.06.01.446579; this version posted June 1, 2021. The copyright holder for this preprint (which was not certified by peer review) is the author/funder, who has granted bioRxiv a license to display the preprint in perpetuity. It is made available under aCC-BY-NC 4.0 International license.

224 cells, we consistently observed decreased cell-to-cell transmission of SARS-CoV-
225 2 compared with a continually increasing trend for SARS-CoV **(Figure 4A and**
226 **Figure 4B)**. This pattern of cell-to-cell transmission was different from that of cell-
227 free infection, where both SARS-CoV-2 and SARS-CoV exhibited an increase, with
228 similar kinetics, in a strictly ACE2 dose-dependent manner (**Figure 4A and Figure**
229 **4B)**. We confirmed ACE2 expression in target cells by flow cytometry and western
230 blotting (**Figure S2A and Figure S2B**). Consistent with increasing expression of
231 ACE2 in target cells, we observed increasing sizes of syncytia formation for SARS-
232 CoV-2, but cell-cell fusion by SARS-CoV was not evident (**Figure S2C**). Giant
233 syncytia formation at 1.5 μg ACE2 resulted in cell death, which might have
234 contributed to decreased cell-to-cell transmission for SARS-CoV-2 (**Figure S2C**).
235 Overall, these results indicate that ACE2 enhances cell-to-cell transmission of both
236 SARS-CoV-2 and SARS-CoV, yet the former requires less ACE2 for the process
237 to occur.

238 We further explored if cell-to-cell transmission of SARS-CoV-2 can occur in
239 the absence of ACE2 expression in target cells. We first used NCI-H520, a human
240 lung epithelial cell line that expresses an extremely low level of ACE2 (**Figure S2D**).
241 Cell-to-cell transmission was detected at day 2, which continued to increase
242 through day 4. In contrast, cell-free infection was not detected in NCI-H520 cells
243 throughout the 3-day period (**Figure 4C**). Cell-to-cell transmission of SARS-CoV
244 was also observed in H520 cells, at a higher level than that of SARS-CoV-2; again,

bioRxiv preprint doi: https://doi.org/10.1101/2021.06.01.446579; this version posted June 1, 2021. The copyright holder for this preprint (which was not certified by peer review) is the author/funder, who has granted bioRxiv a license to display the preprint in perpetuity. It is made available under aCC-BY-NC 4.0 International license.

245 similar to SARS-CoV-2, no/low cell-free infection was detectable (**Figure 4D**). We
246 next tested human PBMCs, which do not express ACE2 (**Figure S2D**), and
247 observed apparent cell-to-cell transmission for both SARS-CoV and SARS-CoV-2,
248 yet no/low cell-free infection was detected, the latter being consistent with recently
249 published results (Banerjee et al., 2020) (**Figure 4E and Figure 4F**). As a control,
250 we carried out cell-to-cell transmission and cell-free infection in Calu-3, a human
251 lung epithelial cell line which expresses a high level of ACE2 (**Figure S2D**). A rapid
252 increase in cell-to-cell transmission was observed for SARS-CoV-2 from day 2
253 through day 4, despite an overall level of infection for SARS-CoV that was higher
254 than observed for SARS-CoV-2 (**Figure S2E and Figure S2F**). Together, these
255 results demonstrated that cell-to-cell transmission of SARS-CoV-2 and SARS-CoV
256 can occur in the absence of ACE2.
257
258 **Cell-to-cell transmission of SARS-CoV-2 involves endosomal entry.** SARS-
259 CoV-2 uses different pathways for entry, either at the plasma membrane and/or in
260 the endosomal compartment (Harrison et al., 2020; Hoffmann et al., 2020; Murgolo
261 et al., 2021; V'Kovski et al., 2021; Wrapp et al., 2020; Yeung et al., 2021). While
262 our results indicated that entry via the plasma membrane is important for cell-to-
263 cell transmission, we probed whether fusion in the endosomal compartment may
264 also be involved. We applied in parallel a panel of endosomal inhibitors to the cell-
265 to-cell and cell-free infection assays. We found that cathepsin L inhibitor III,

bioRxiv preprint doi: https://doi.org/10.1101/2021.06.01.446579; this version posted June 1, 2021. The copyright holder for this preprint (which was not certified by peer review) is the author/funder, who has granted bioRxiv a license to display the preprint in perpetuity. It is made available under aCC-BY-NC 4.0 International license.

266 cathepsin B inhibitor CA-074, E-64d (general cathepsin inhibitor), BafA1 (ATPase
267 pump inhibitor), and Leupeptin (general protease inhibitor), all significantly
268 inhibited cell-to-cell transmission (**Figure 5A**). Interestingly, the effect of these
269 drugs on SARS-CoV-2 were generally less potent compared to SARS-CoV, with
270 the exception of cathepsin L inhibitor III (**Figure 5A**). Moreover, these drugs
271 generally showed a stronger effect on cell-free infection, again especially for
272 SARS-CoV (**Figure 5B**). Of note, CA-074 had modest effects on both viruses
273 (**Figure 5B**), which was consistent with the notion that cathepsin B does not play
274 a significant role in cleaving the spike protein of SARS-CoV and SARS-CoV-2,
275 which is required for fusion (Nitulescu et al., 2020; Ou et al., 2020). We also applied
276 these inhibitors to cell-cell fusion assays but found no effect on either SARS-CoV-
277 2 or SARS-CoV, as would be expected (**Figure S3**). To assess possible cell type-
278 dependent effects, we carried out experiments using Caco-2 target cells and found
279 that cathepsin L inhibitor III and BafA1 robustly inhibited cell-to-cell transmission
280 and cell-free infection of both viruses, in particular SARS-CoV (**Figure 5C and**
281 **Figure 5D)**. Overall, these results support the notion that endosomal entry is
282 involved in cell-to-cell transmission of SARS-CoV-2, and to a greater extent,
283 SARS-CoV.
284
285 **Cell-to-cell transmission of SARS-CoV-2 is refractory to neutralizing**
286 **antibody and convalescent plasma.** One important feature of the virus cell-to-

bioRxiv preprint doi: https://doi.org/10.1101/2021.06.01.446579; this version posted June 1, 2021. The copyright holder for this preprint (which was not certified by peer review) is the author/funder, who has granted bioRxiv a license to display the preprint in perpetuity. It is made available under aCC-BY-NC 4.0 International license.

287 cell transmission is evasion of host immunity, particularly neutralizing antibody-
288 mediated response. We therefore examined the sensitivity of SARS-CoV-2 spike-
289 mediated cell-to-cell transmission to neutralization by a monoclonal antibody
290 against the receptor-binding domain of the spike, 2B04 (Alsoussi et al., 2020), as
291 well as convalescent plasma derived from COVID-19 patients (Roback and
292 Guarner, 2020; Zeng et al., 2020). While 2B04 effectively inhibited cell-free
293 infection of SARS-CoV-2 in 293T/ACE2 cells by more than 90%, its effect on cell-
294 to-cell transmission between 293T and 293T/ACE2 was ~50% (**Figure 6A and**
295 **Figure 6B**). As would be expected, 2B04 had no effect on SARS-CoV, regardless
296 of cell-to-cell transmission or cell-free infection (**Figure 6A and Figure 6B**). We
297 also performed cell-cell fusion in the presence of different concentrations of 2B04,
298 and we found that the fusion activity of the SARS-CoV-2 spike was inhibited in a
299 dose-dependent manner (**Figure 6C**). We then tested five serum samples of
300 COVID-19 patients, and observed that, although they potently inhibited the cell-
301 free infection of SARS-CoV-2 ($p<0.001$), they showed variable but no significant
302 effect on cell-to-cell transmission of SARS-CoV-2; the effect of these sera on
303 SARS-CoV infection, either cell-to-cell or cell-free, was minimal or modest (**Figure**
304 **6D and 6E)**. Together, these results indicate that cell-to-cell transmission of SARS-
305 CoV-2 is mostly refractory to neutralization by neutralizing antibodies against spike
306 relative to cell-free infection.
307

bioRxiv preprint doi: https://doi.org/10.1101/2021.06.01.446579; this version posted June 1, 2021. The copyright holder for this preprint (which was not certified by peer review) is the author/funder, who has granted bioRxiv a license to display the preprint in perpetuity. It is made available under aCC-BY-NC 4.0 International license.

308 **Cell-to-cell transmission of SARS-CoV-2 variants of concern and their**
309 **sensitivity to COVID-19 vaccinee sera.** The D614G mutation in SARS-CoV-2
310 spike, as well as emerging variants of concern (VOCs) containing D614G and
311 other key spike mutations, have been reported to enhance viral infectivity,
312 transmissibility, and resistance to COVID-19 vaccines (Khan et al., 2021; Noh et
313 al., 2021; Plante et al., 2021; Wu et al., 2021; Xie et al., 2021; Zhou et al., 2021).
314 As such, we examined the cell-to-cell transmission capability of authentic SARS-
315 CoV-2 WT (USA-WA1/2020), D614G variant (B.1.5), and two VOCs B.1.1.7
316 (501Y.V1) and B.1.351 (South African, 501Y.V2), in the presence or absence of
317 pooled sera from mRNA vaccinees (3 Moderna and 3 Pfizer). Donor Vero-ACE2
318 cells were first infected with WT SARS-CoV-2 (MOI=0.2), D614G (MOI=0.02),
319 B.1.1.7 (MOI=0.02), and B.1.351 (MOI=0.02), respectively. Note that a 10-fold
320 higher MOI was used for WT in order to achieve comparable rates of infection in
321 donor cells between WT and VOCs, given that D614G-containing variants are
322 known to significantly increase the viral infectivity (Plante et al., 2021; Zhang et al.,
323 2020a). Approximately 20 hrs post-infection, the culture media of donor cells was
324 harvested, of which the whole volume of which was used to infect target Vero-
325 mTomato-Red cells for 6 hr in order to determine the viral infectivity. In parallel,
326 the infected donor Vero-ACE2 cells were digested, and cocultured with the same
327 number of Vero-Tomato-Red cells as was used in the cell-free infectivity assay,
328 also for 6 hrs, as a measurement of cell-to-cell transmission. To determine the

bioRxiv preprint doi: https://doi.org/10.1101/2021.06.01.446579; this version posted June 1, 2021. The copyright holder for this preprint (which was not certified by peer review) is the author/funder, who has granted bioRxiv a license to display the preprint in perpetuity. It is made available under aCC-BY-NC 4.0 International license.

329 sensitivity of cell-to-cell transmission vs. cell-free infection to neutralization by
330 vaccinee sera, we pooled the serum samples of 6 mRNA vaccinees, i.e., 3 from
331 Moderna and 3 from Pfizer, and added them to the cultured medium. The efficiency
332 of cell-to-cell transmission and cell-free infectivity was determined by measuring
333 the percentage of SARS-CoV-2 nucleocapsid (N)-positive Vero-mTomato-Red
334 cells using flow cytometry. Considering the potential impact of infected donor cells
335 on cell-to-cell transmission, we normalized the rate of cell-to-cell transmission with
336 the total rate of virus spread in both SARS-CoV-2-positive Vero-mTomato-Red
337 cells as well as Vero-ACE2 cells over the entire infection period, i.e., from the initial
338 infection of donor cells to the end of coculture (~26 hrs).

339 Representative flow cytometric results and summary analyses are presented
340 in **Figure 7** and **Figure S4**. Interestingly, even with a 10-fold higher MOI used for
341 the WT infection of donor Vero-ACE2 cells relative to other variants, we observed
342 comparable rates of cell-to-cell transmission between WT, D614G, B.1.1.7, and
343 B.1.351 (**Figure 7A,** upper panel; **Figure 7B** and **Figure S4A**). Note that the
344 relative rate of cell-to-cell transmission shown in **Figure 7B** was obtained by
345 dividing the percentage of SARS-CoV-2-positive Vero-mTomato-Red cells (*Q2* in
346 **Figure 7A,** upper panel) by the percentage of total SARS-CoV-2-positive cells (Q2
347 plus *Q3* in **Figure 7A,** upper panel). We noted that the rate of B.1.351 spreading
348 infection in Vero-ACE2 and Vero-mTomato-Red cells (Q2 plus Q3 in **Figure A**,
349 upper panel) was the highest, followed by B.1.1.7 > D614G > WT (**Figure 7C**).

bioRxiv preprint doi: https://doi.org/10.1101/2021.06.01.446579; this version posted June 1, 2021. The copyright holder for this preprint (which was not certified by peer review) is the author/funder, who has granted bioRxiv a license to display the preprint in perpetuity. It is made available under aCC-BY-NC 4.0 International license.

350 Consistent with the more efficient replication of B.1.351 in donor Vero-ACE2 cells
351 over the entire 26 hr infection period (Q3 in **Figure 7A,** upper panel), we found a
352 significantly higher cell-free infectivity for B.1.351 produced during the initial 20-hr
353 infection relative to WT, D614G and B.1.1.7 (**Figure 7D,** see “no sera”). Overall,
354 these results revealed a strongly enhanced replication of B.1.351 relative to
355 B.1.1.7, D614G and WT, yet a comparable efficiency of cell-to-cell transmission
356 between WT, D614G and VOCs.

357 We also assessed the sensitivity of cell-to-cell transmission and cell-free
358 infection to neutralization by Moderna and Pfizer vaccinee sera. With a relatively
359 low dose of pooled sera being applied, we observed that the cell-to-cell
360 transmission of WT, D614G, B.1.1.7 and B.1.351 was virtually resistant to
361 neutralizing antibodies induced by these mRNA vaccinees for all viruses, whereas
362 the cell-free infection of WT, D614G and B.1.1.7 was strongly inhibited, with
363 B.1.351 being resistant (**Figure 7A**, lower panels; **Figure 7D and Figure 7E;**
364 **Figure S4B and Figure S4C**). By using HIV-inGluc pseudotyped viruses with
365 serially diluted serum samples from Moderna and Pfizer vaccinees, we were able
366 to obtain and compare the NT_{50} values of each virus in cell-to-cell transmission vs.
367 cell-free infection. We found that, overall, mRNA vaccinee sera neutralized cell-to-
368 cell transmission approximately 3-fold less efficiently than cell-free infection, with
369 the notable exception of B.1.351, which showed similar extents of inhibition for cell-
370 to-cell and cell-free infections (**Figure 7F and Figure 7G**). Intriguingly, we found

bioRxiv preprint doi: https://doi.org/10.1101/2021.06.01.446579; this version posted June 1, 2021. The copyright holder for this preprint (which was not certified by peer review) is the author/funder, who has granted bioRxiv a license to display the preprint in perpetuity. It is made available under aCC-BY-NC 4.0 International license.

371 that the cell-to-cell transmission of B.1.1.7 was more resistant to neutralization by
372 vaccine sera, with ~4.9-fold lower NT_{50} than D614G (p<0.01) and ~8.7-fold lower
373 than B.1.351 (p<0.05) (**Figure 7F and Figure 7G**). In contrast, the cell-free
374 infection of B.1.351 was more resistant to neutralization than D614G and B.1.1.7,
375 with 3.6-fold (p<0.01) and ~2.4-fold (p<0.01) lower NT_{50}, respectively (**Figure 7F**
376 **and Figure 7G**), which was consistent with recent studies (Planas et al., 2021;
377 Wang et al., 2021). In aggregate, these results confirmed that cell-to-cell
378 transmission of both authentic and pseudotyped SARS-CoV-2 VOCs is more
379 refractory to inhibition by neutralizing antibodies induced by mRNA vaccines as
380 compared to cell-free infection, and more importantly, showed that the cell-to-cell
381 transmission of B.1.1.7 and the cell-free infection of B.1.351, are most resistant to
382 the antibody neutralization. The differential sensitivity of B.1.1.7 and B.1.351 to
383 neutralization by vaccinee sera in cell-to-cell transmission vs cell-free infection
384 likely has important implications for understanding the spread of these variants and
385 their pathogenesis in patients (see Discussion).
386

387 **Discussion**

388 Accumulating evidence indicates that viruses, including the highly pathogenic
389 HIV, HCV, and EBOV, etc., can efficiently spread through cell-to-cell transmission
390 (Cifuentes-Munoz et al., 2018; Dale et al., 2013; Miao et al., 2016; Sattentau, 2008;
391 Wang et al., 2017; Xiao et al., 2014; Zhong et al., 2013a). Importantly, cell-to-cell

bioRxiv preprint doi: https://doi.org/10.1101/2021.06.01.446579; this version posted June 1, 2021. The copyright holder for this preprint (which was not certified by peer review) is the author/funder, who has granted bioRxiv a license to display the preprint in perpetuity. It is made available under aCC-BY-NC 4.0 International license.

392 transmission is more efficient than cell-free infection (Zhong et al., 2013a), and
393 roles for this mode of transmission have been demonstrated in vivo for HIV and
394 other viruses (Agosto et al., 2014; Dale et al., 2013; Xiao et al., 2014; Zhong et al.,
395 2013a). Notably, many plant viruses are known to use cell-to-cell transmission to
396 spread from epidermal cells and move sequentially into mesophyll, bundle sheath,
397 and phloem parenchyma and companion cells (Carrington et al., 1996; Hipper et
398 al., 2013). For coronaviruses, very little is currently known about their mode of
399 spread between cells or its efficiency compared to cell-free infection. This question
400 is critical, given the robust replication of SARS-CoV-2 in human lung and other
401 tissues, as well as the rapid spread of SARS-CoV-2, including some variants of
402 concern, in the human population, leading to the global pandemic (Chu et al., 2020;
403 Grubaugh et al., 2021; Planas et al., 2021; Walensky et al., 2021; Wang et al.,
404 2021). In this work, we addressed this question using lentiviral pseudotypes and
405 replication-competent rVSV expressing the spike of SARS-CoV-2 or SARS-CoV.
406 We discovered that SARS-CoV-2 spike is more efficient in mediating cell-to-cell
407 transmission than SARS-CoV spike, yet the spike of SARS-CoV is more capable
408 of mediating cell-free infection. To our knowledge, this is the first direct comparison
409 of cell-to-cell transmission vs. cell-free infection between SARS-CoV-2 and SARS-
410 CoV in cultured cells, and the results provide important insights into two distinct
411 modes of infection and the host-viral factors that regulate these processes.

bioRxiv preprint doi: https://doi.org/10.1101/2021.06.01.446579; this version posted June 1, 2021. The copyright holder for this preprint (which was not certified by peer review) is the author/funder, who has granted bioRxiv a license to display the preprint in perpetuity. It is made available under aCC-BY-NC 4.0 International license.

412 Why is SARS-CoV-2 spike more efficient than SARS-CoV spike for mediating
413 cell-to-cell transmission in cultured cells? We provide evidence that this is in part
414 related to the higher cell-cell fusion activity of SARS-CoV-2 spike compared to
415 SARS-CoV (Figure 2). However, we also recognized that extensive cell-cell fusion
416 by SARS-CoV-2 spike can lead to giant syncytia formation and cell death, which
417 in turn reduces cell-to-cell transmission. Therefore, fine control of the spike-
418 induced cell-cell fusion is important for efficient cell-to-cell transmission and,
419 therefore, the spreading infection of SARS-CoV-2. Further evidence supporting a
420 role of cell-cell fusion in transmission of SARS-CoV-2 came from the application
421 of a membrane fusion inhibitor EK1, which significantly attenuated cell-to-cell
422 transmission. Interestingly, although ACE2 enhances cell-to-cell transmission of
423 SARS-CoV-2 and SARS-CoV, we found that it is not absolutely required. This
424 observation is supported further by data from H520 cells and human PBMCs,
425 which express a minimal level of ACE2 if any, yet exhibited obvious cell-to-cell
426 transmission (Figure 4). Cell-free infection of SARS-CoV-2 was not detected in
427 H520 cells and PBMCs, further supporting these conclusions. The molecular
428 mechanism underlying cell-to-cell transmission of SARS-CoV-2, including the
429 possible roles of cellular cofactors and virological synapses, shall be investigated
430 in future studies.

431 A surprising result to emerge from our studies was that, despite the critical
432 role of cell-cell contact and plasma membrane-mediated fusion, endosomal entry

bioRxiv preprint doi: https://doi.org/10.1101/2021.06.01.446579; this version posted June 1, 2021. The copyright holder for this preprint (which was not certified by peer review) is the author/funder, who has granted bioRxiv a license to display the preprint in perpetuity. It is made available under aCC-BY-NC 4.0 International license.

433 pathways were also involved in cell-to-cell transmission of SARS-CoV-2 and
434 SARS-CoV (Figure 5). This is evidenced by the inhibitory effect of drugs that
435 specifically target the endosomal entry pathway of these viruses, including the
436 CatL inhibitor III, which blocks cleavage of the viral glycoprotein, as well as BafA1,
437 which neutralizes endosomal pH. These results are reminiscent of previous studies
438 from HIV and EBOV, where endocytosis and/or protease cleavage are required for
439 cell-to-cell transmission of these enveloped viruses (Dale et al., 2011; Markosyan
440 et al., 2016; Miao et al., 2016; Titanji et al., 2013; Wang et al., 2017). Interestingly,
441 we find that these inhibitors appear to be less potent for decreasing cell-to-cell
442 transmission as compared to cell-free infection, and moreover, their effects on
443 SARS-CoV-2 are less than their effects on SARS-CoV. These observations
444 collectively suggest a less dominant role for the endosomal entry pathway in cell-
445 to-cell transmission of SARS-CoV-2. High-resolution live microscopic imaging
446 would be useful to dissect the exact role of endosomal vs. plasma entry pathway
447 in the cell-to-cell transmission of SARS-CoV-2.

448 Cell-to-cell transmission is considered to be an effective means by which
449 viruses evade host immunity, especially antibody-mediated responses. We
450 compared the sensitivity of cell-to-cell transmission vs. cell-free infection of SARS-
451 CoV-2 to treatments by neutralizing monoclonal antibodies and COVID-19
452 convalescent plasma - both of which have been approved by the FDA for
453 emergency use. We found that while cell-free infection of SARS-CoV-2 was almost

bioRxiv preprint doi: https://doi.org/10.1101/2021.06.01.446579; this version posted June 1, 2021. The copyright holder for this preprint (which was not certified by peer review) is the author/funder, who has granted bioRxiv a license to display the preprint in perpetuity. It is made available under aCC-BY-NC 4.0 International license.

454 completely blocked by these treatments, cell-to-cell transmission of SARS-CoV-2
455 was, to a large extent, refractory (Figures 6 and 7). While not statistically significant,
456 some of the COVID-19 sera (2 out of 5) even enhanced cell-to-cell transmission of
457 SARS-CoV-2 (Figure 6D), although the underlying mechanisms are currently not
458 known. Interestingly, despite significant increases in cell-free infectivity, the South
459 Africa variant B.1.351, the UK variant B.1.1.7, as well as the D614G variant,
460 exhibited similar efficiencies of cell-to-cell transmission compared with the WT
461 (Figure 7). Moreover, although B.1.351 is more resistant to vaccinee sera in cell-
462 free infection, consistent with some recent reports (Planas et al., 2021; Wang et
463 al., 2021), B.1.1.7 seems more resistant to the vaccinee sera for the cell-to-cell
464 transmission route (Figure 7), may explain that B.1.1.7 has longer duration of acute
465 infection than others (Kissler et al., 2021). The mechanism underlying these
466 observations is currently unclear, but may have implications for understanding the
467 rapid spread of VOCs in human population as well as their increased pathogenesis.
468 The cell-free route is directly linked to the ability of viruses to infect target cells and
469 result in spreading among humans through person-to-person contact. In contrast,
470 cell-to-cell transmission has dominant roles in viral pathogenesis and disease
471 progression (Mothes et al., 2010). Thus, our results on the resistance of B.1.1.7
472 and B.1.351 to vaccinee sera-mediated inhibition of cell-to-cell transmission and
473 cell-free infection may provide molecular and virological underpinnings for the
474 prolonged viral replication and rapid spread of these two variants in the world

bioRxiv preprint doi: https://doi.org/10.1101/2021.06.01.446579; this version posted June 1, 2021. The copyright holder for this preprint (which was not certified by peer review) is the author/funder, who has granted bioRxiv a license to display the preprint in perpetuity. It is made available under aCC-BY-NC 4.0 International license.

475 population (Alpert et al., 2021; Funk et al., 2021; Planas et al., 2021; Wang et al.,
476 2021).
477

478 **Limitations of the Study**

479 While in this work, we obtained evidence that SARS-CoV-2 spike more
480 efficiently mediates cell-to-cell transmission than the SARS-CoV spike, a direct
481 comparison using authentic viruses of both, especially in primary human lung and
482 airway epithelial cells, is needed. As an initial step toward this goal, we have
483 attempted to apply rVSV-GFP-SARS-CoV-2 and rVSV-GFP-SARS-CoV to human
484 primary bronchial and nasal epithelial cell cultures, but the efficiency of spread for
485 both viruses was too low to draw any conclusion. Although in this work, we
486 examined roles of ACE2 and endosomal proteases in cell-to-cell transmission vs.
487 cell-free infection, how other host cofactors, including TMPRSS2, modulate this
488 process will need to be investigated. Ultimately, we must determine the role, if any,
489 of cell-to-cell transmission of SARS-CoV-2 in disease progression and
490 pathogenesis in COVID-19 patients.
491

492 **ACKNOWLEDGEMENTS**

493 We thank Gerard Lozanski, Richard Gumina, Eric Freed, David Derse, Marc
494 Johnson, Fang Li, and Ali Ellebedy for provision of sera samples, plasmids, and
495 cells. We also thank the NIH AIDS Reagent Program and BEI Resources for

bioRxiv preprint doi: https://doi.org/10.1101/2021.06.01.446579; this version posted June 1, 2021. The copyright holder for this preprint (which was not certified by peer review) is the author/funder, who has granted bioRxiv a license to display the preprint in perpetuity. It is made available under aCC-BY-NC 4.0 International license.

496 supplying important reagents that made this work possible. This work was
497 supported by a fund provided by an anonymous private donor to The Ohio State
498 University and NIH grant U54CA260582; additional support of SLL's lab includes
499 NIH grants R01 AI112381 and R01 AI150473. The content is solely the
500 responsibility of the authors and does not necessarily represent the official views
501 of the NIH. LJS was partially supported by NIH grant NICHD R01 HD095881.

502

503 **Author contributions**: SLL conceived and led the project. CZ performed majority
504 of the presented experiments. JPE designed the construction of variants of
505 concern and performed part of the neutralization assay. TK performed rVSV-GFP
506 spread experiments in human airway epithelial cells. YMZ produced rVSV viruses
507 and sequenced the spike gene. SPJW contributed to the rVSV stock. CZ, JPE, TK,
508 YMZ, GO, SPJW, LS, MEP and SLL all contributed to data analyses and
509 discussion. CZ and SLL wrote the paper, which was edited and approved by all
510 coauthors.

511

512 **Competing interests**: No.

513

514 **Figure legends**

515

516 **Figure 1. The spike protein of SARS-CoV-2 and SARS-CoV mediates cell-to-**
517 **cell transmission of HIV-1 lentiviral pseudotypes. (A and B)** Schematic

bioRxiv preprint doi: https://doi.org/10.1101/2021.06.01.446579; this version posted June 1, 2021. The copyright holder for this preprint (which was not certified by peer review) is the author/funder, who has granted bioRxiv a license to display the preprint in perpetuity. It is made available under aCC-BY-NC 4.0 International license.

518 representations of cell-to-cell and cell-free infection assays (see details in
519 Methods). Briefly, the inGluc-based lentiviral pseudotypes bearing spike were
520 produced in 293T cells, which were cocultured with the target cells (293T/ACE2)
521 for cell-to-cell transmission; the Gluc activity of cocultured cells was measured over
522 time (**A**). Cell-free infection was performed by harvesting virus from the same
523 number of producer cells, followed by infecting 293T/ACE2 target cells in the
524 presence of the same number of untransfected 293T cells; alternatively, cell-free
525 infection was carried out in *transwell* plates, from which Gluc activity was
526 measured (**B**). **(C)** Comparison of cell-to-cell transmission mediated by SARS-
527 CoV-2 or SARS-CoV spike. Results shown were from 6 independent experiments,
528 with cell-free infection measured at 48 and 72 hr after coculture; the portion of cell-
529 free infection was excluded (n=6). **(D)** Comparison of cell-free infection mediated
530 by SARS-CoV-2 or SARS-CoV spike. Results were from 6 independent
531 experiments (n=6). **(E)** The expression level of spike proteins on the plasma
532 membrane of donor cells was measured by flow cytometry using a polycolonal
533 antibody T62, which detects both SARS-CoV-2 and SARS-CoV. **(F and G)** The
534 calculated ratios between cell-to-cell and cell-free infection mediated by SARS-
535 CoV-2 or SARS-CoV-2 spike. Results from cell coculture were shown in (F) and
536 from *transwell* plates were shown in (G) (n=3~6).
537

bioRxiv preprint doi: https://doi.org/10.1101/2021.06.01.446579; this version posted June 1, 2021. The copyright holder for this preprint (which was not certified by peer review) is the author/funder, who has granted bioRxiv a license to display the preprint in perpetuity. It is made available under aCC-BY-NC 4.0 International license.

538 **Figure 2. rVSV expressing SARS-CoV-2 spike spreads faster than does rVSV**
539 **bearing SARS-CoV spike.** Vero-E6 cells were infected with rVSV-GFP-SARS-
540 CoV-2 or SARS-CoV (MOI=0.01); 1 h post-infection, cells were washed with PBS
541 and cultured in the presence of 1% methylcellulose. Photos were taken at 18 h
542 and 24 h **(A)**. After 72 hrs infection, cells were fixed with 3.7% PFA and stained
543 with crystal violet **(B)**. The number and size of plaques were plotted in **(C) and (D),**
544 respectively.
545
546 **Figure 3**. **Cell-cell fusion mediated by SARS-CoV and SARS-CoV-2 spike**
547 **contributes to cell-to-cell transmission. (A)** Syncytia formation mediated by the
548 spike of SARS-CoV-2 or SARS-CoV. 293T donor cells were cotransfected with
549 plasmids encoding SARS-CoV-2 or SARS-CoV spike, lentiviral NL4-3 inGluc
550 vector and eGFP. After 24 h post-transfection, the donor cells were cocultured with
551 target 293T/ACE2 cells at 1:1 ratio, with fusion monitored over time and photos
552 taken after 2 hr and 24 hr, respectively. **(B)** Quantification of cell-cell fusion. 293T
553 cells were transfected with plasmids encoding tet-off or SARS-CoV or SARS-CoV-
554 2 spike and were cocultured with target 293FT-mCAT-Gluc cells, which were
555 transfected with a plasmid expressing ACE2; Gluc activity was measured from the
556 supernatant of cocultured cells at 24 hr and 48 hr, respectively. Relative fusion
557 was plotted by setting the fusion activity of SARS-CoV as 1.0. **(C, D and E)** Fusion
558 inhibitor EK1 inhibits cell-cell fusion of SARS-CoV-2 spike, in accordance with its

bioRxiv preprint doi: https://doi.org/10.1101/2021.06.01.446579; this version posted June 1, 2021. The copyright holder for this preprint (which was not certified by peer review) is the author/funder, who has granted bioRxiv a license to display the preprint in perpetuity. It is made available under aCC-BY-NC 4.0 International license.

559 effect on cell-to-cell transmission. Effect of EK1 on syncytia formation induced by
560 SARS-CoV-2 spike (**C**); photos were taken at 24 hr. Effects of EK1 on SARS-CoV-
561 2 or SARS-CoV infection from 293T to 293T/ACE2 **(D)** or from 293T to Caco-2 **(E)**.
562 Transfected 293T donor cells were cocultured with 293T/ACE2 or Caco-2 cells in
563 the presence or absence of 10 μM EK1 and Gluc activity was measured at 24 to
564 72 hr after coculture. Results from 3 to 6 independent experiments were averaged
565 and plotted as relative values by setting the mock control as 100% (n=3~6).
566
567 **Figure 4**. **ACE2 enhances cell-to-cell transmission but is not absolutely**
568 **required**. (**A and B**) Cell-to-cell and cell-free infection was performed as
569 described for Figures 1 and 3 except that target cells were 293T transfected with
570 different amounts of a plasmid encoding ACE2. Relative rates of cell-to-cell
571 transmission and cell-free infection were calculated by setting the values of 0.5 μg
572 ACE2 to 1.0 **(A and B,** n=3**).** (**C, D, E and F**) Experiments were carried out as
573 described for Figures 1 and 3 except that target cells were H520 and human
574 PBMCs (n=3 for each).
575
576 **Figure 5. Endosomal entry pathway is involved in cell-to-cell transmission.**
577 Effect of endosomal entry inhibitors on cell-to-cell and cell-free infection of SARS-
578 CoV-2 and SARS-CoV. Experiments were carried out as described in Figures 1C
579 and 1D, except that indicated inhibitors were present during the infection period.

bioRxiv preprint doi: https://doi.org/10.1101/2021.06.01.446579; this version posted June 1, 2021. The copyright holder for this preprint (which was not certified by peer review) is the author/funder, who has granted bioRxiv a license to display the preprint in perpetuity. It is made available under aCC-BY-NC 4.0 International license.

580 The concentrations of inhibitors used were as follows: 1 μM or 5 μM Cat L inhibitor
581 III, 1 μM or 5 μM CA-074, 10 μM or 30 μM E-64D, 25 nM or 50 nM BafA1, and 20
582 μM or 50 μM leupeptin. **(A and B**) Effect in 293T cells. **(C and D)** Effect in Caco-2
583 cells. In all experiments, Gluc activity was measured at 48 and 72 hr after infection,
584 and rates of relative infection were plotted by setting the values of mock infection
585 without drugs to 100. Results were from 4~6 independent experiments.
586
587 **Figure 6. Cell-to-cell transmission of SARS-CoV-2 is refractory to inhibition**
588 **by neutralizing antibody and COVID-19 convalescent plasma. (A, B and C)**
589 Effects of SARS-CoV-2 monoclonal antibody 2B04 on cell-to-cell transmission,
590 cell-free infection, and cell-cell fusion mediated by SARS-CoV-2 or SARS-CoV-2
591 spike. The experiments were carried out as described in Figures 1C and 1D,
592 except that 0.2 μg/mL or 2 μg/mL 2B04 were included during the infection period.
593 Relative infections were plotted by setting the values of mock infection without
594 2B04 to 100% for statistical analyses (**A and B**). The photos of syncytia formation
595 were taken at 18 h after coculture and presented (**C**). **(D and E)** Effect of COVID-
596 19 sera on cell-to-cell and cell-free infection of SARS-CoV-2 and SARS-CoV.
597 Experiments were performed as described as above, except five diluted COVID-
598 19 sera were included during the infection period. Effect on cell-to-cell **(D)** and cell-
599 free **(E)** of SARS-CoV or SARS-CoV-2 were summarized and plotted by setting
600 the values of mock infection control to 100% (n=3~4).

bioRxiv preprint doi: https://doi.org/10.1101/2021.06.01.446579; this version posted June 1, 2021. The copyright holder for this preprint (which was not certified by peer review) is the author/funder, who has granted bioRxiv a license to display the preprint in perpetuity. It is made available under aCC-BY-NC 4.0 International license.

601

602 **Figure 7. Cell-to-cell transmission of SARS-CoV-2 VOCs and sensitivity to**
603 **neutralization by vaccinee sera. (A-E)** The cell-to-cell transmission capability of
604 authentic SARS-CoV-2 WT, D614G, B.1.1.7 and B.1.351 in the presence or
605 absence of vaccinee sera. Donor Vero-ACE2 cells were infected with WT SARS-
606 CoV-2 (MOI=0.2), D614G (MOI=0.02), B.1.1.7 (MOI=0.02), and B.1.351
607 (MOI=0.02) for 20 hr, followed by coculturing with target Vero-mTomato (Red) cells
608 in the presence or absence of pooled mRNA vaccinee sera (3 Moderna and 3
609 Pfizer) for 6 hr. Cells were fixed and stained with anti-SARS-CoV-2 N protein, and
610 analyzed by flow cytometry. Representative flow cytometric analyses of infected
611 cells were shown in (**A**), with the newly infected target Vero-mTomato (Red) cells
612 (Q2) as indicative of cell-to-cell transmission. The relative cell-to-cell transmission
613 efficiency was calculated by dividing the rate of Vero-mTomato-Red positive cells
614 (Q2) by the rate of total infected donor and target cells (Q2+Q3) (**B,** n=3). The MOI-
615 normalized total viral spread in both donor and target cells (Q2+Q3) was shown in
616 **(C)** (n=3). The supernatant from the initial 20 hr infection of donor cells was used
617 to infect target Vero-mTomato-Red cells for 6 hr as the measurement of cell-free
618 viral infectivity, either in the presence or absence of the pooled vaccinee sera, and
619 infected cells were analyzed by flow cytometry **(D)** (n=3). The pooled vaccinee
620 sera were also added to the cocultured Vero-ACE2 and Vero-mTomato-Red cells
621 as described in (**A**) to determine their effect on cell-to-cell transmission **(E)**. **(F and**

bioRxiv preprint doi: https://doi.org/10.1101/2021.06.01.446579; this version posted June 1, 2021. The copyright holder for this preprint (which was not certified by peer review) is the author/funder, who has granted bioRxiv a license to display the preprint in perpetuity. It is made available under aCC-BY-NC 4.0 International license.

622 **G)** The calculated NT_{50} values of vaccine sera against cell-to-cell transmission and
623 cell-free infection of lentiviral pseudotypes bearing individual spike of VOCs.
624 Experimental procedures were the same as described in Figures 6D and 6E,
625 except that all comparisons were made relative to the D614G variant (n=6).

626

627 # STAR★METHODS

628 ## LEAD CONTACT AND MATERIALS AVAILABILITY

629 Further information and requests for resources and reagents should be directed to
630 and will be fulfilled by the Lead Contact, Shan-Lu Liu (liu.6244@osu.edu).

631 ## EXPERIMENTAL MODEL AND SUBJECT DETAILS

632 **Cell culture.** 293T (ATCC CRL-11268, RRID: CVCL_1926), Vero-E6 (ATCC CRL-
633 1586, RRID: CVCL_0574) and Vero-ACE2 (Vero-E6 expressing high endogenous
634 ACE2, BEI, NR-53726) cells were grown in Dulbecco's modified Eagle's medium
635 (DMEM) supplemented with 1% penicillin/streptomycin and 10% (vol/vol) fetal
636 bovine serum (Thermo Fisher Scientific). Caco-2 (ATCC HTB-37, RRID:
637 CVCL_0025) cells were grown in Dulbecco's modified Eagle's medium (DMEM)
638 supplemented with 1% penicillin/streptomycin and 20% (vol/vol) FBS. Calu-3 cells

bioRxiv preprint doi: https://doi.org/10.1101/2021.06.01.446579; this version posted June 1, 2021. The copyright holder for this preprint (which was not certified by peer review) is the author/funder, who has granted bioRxiv a license to display the preprint in perpetuity. It is made available under aCC-BY-NC 4.0 International license.

639 (ATCC HTB-55, RRID: CVCL_0609) were grown in Eagle's Minimum Essential
640 Medium (EMEM) supplemented with 1% penicillin/streptomycin and 10% (vol/vol)
641 FBS. Human peripheral blood mononuclear cells (PBMCs) were gifts of Eric O.
642 Freed (National Cancer Institute, Frederick, Maryland, USA) and maintained in
643 Roswell Park Memorial Institute (RPMI) 1640 Medium containing 10% (vol/vol)
644 FBS. NCI-H520 (ATCC HTB-182, RRID: CVCL_1566) cells were grown in RPMI
645 1640 Medium supplemented with 1% penicillin/streptomycin and 10% (vol/vol)
646 fetal bovine serum. The 293T/ACE2 cell line was obtained from BEI (NR-52511).
647 Vero-E6 cells stably expressing red tomato were generated by transduction of a
648 lentiviral vector expressing the tomato gene, followed by hygromycin B selection
649 (200 µg/mL) for 6 days. All cell lines utilized were maintained at 37°C, 5% CO2.

650 **Virus.** rVSV-GFP-SARS-CoV and rVSV-GFP-SARS-CoV-2 (obtained from Sean
651 Whelan's lab at the Washington University School of Medicine in St. Louis,
652 Missouri, USA) were amplified in Vero-E6 cells and maintained under a humidified
653 atmosphere of 5% CO_2 at 34°C in Dulbecco's modified Eagle's medium (DMEM)
654 supplemented with 10% FBS. The spike sequence in the original stock and each
655 passage was confirmed by DNA sequencing. Authentic SARS-CoV-2 WT (USA-
656 WA1/2020, NR-52281; kindly prepared by Jacob Yount of The Ohio State
657 University, Columbus, Ohio, USA), D614G (B.1.5, NR-53944), B.1.1.7 (501Y.V1,
658 NR-54000) and B.1.351 (501Y.V2, NR-54009) were all obtained from BEI.

bioRxiv preprint doi: https://doi.org/10.1101/2021.06.01.446579; this version posted June 1, 2021. The copyright holder for this preprint (which was not certified by peer review) is the author/funder, who has granted bioRxiv a license to display the preprint in perpetuity. It is made available under aCC-BY-NC 4.0 International license.

659 **METHOD DETAILS**

660 **Constructs, antibodies and reagents.** HIV-1 NL4.3-inGluc was a gift of Marc
661 Johnson at the University of Missouri (Columbia, Missouri, USA). Plasmids
662 pcDNA3.1-SARS-CoV-S-C9 and pcDNA3.1-SARS-CoV2-S-C9 encoding the full-
663 length spike were obtained from Fang Li at the University of Minnesota (St. Paul,
664 Minnesota, USA). A construct for ACE2 transient expression, pHAGE2-ACE2, was
665 obtained from BEI resources (NR-52512). A lentiviral vector encoding red tomato
666 was from Marc Johnson (University of Missouri, Columbia, USA). The codon-
667 optimized D614G, B.1.351 and B.1.1.7 SARS-CoV-2 S constructs were
668 synthesized by GenScript and subsequently cloned into a pcDNA3.1 vector by
669 restriction enzyme cloning with Kpn I and BamH I. Primary antibodies used for
670 western blotting and flow cytometry were anti-coronavirus spike (Sino Biological,
671 40150-T62), anti-SARS-CoV-2 Nucleocapsid (Sino Biological, 40143-MM08), anti-
672 hACE2 (R&D, AF933) and anti-β-actin (Sigma, A1978). Secondary antibodies
673 used for western blotting included anti-Mouse IgG-Peroxidase (Sigma, A5278),
674 anti-Rabbit IgG-Peroxidase (Sigma, A9169) and anti-Goat IgG-Peroxidase (Sigma,
675 A8919). Secondary antibodies used for flow cytometry included anti-Rabbit IgG–
676 FITC (Sigma, F9887), anti-Mouse IgG-FITC (Sigma, F0257), anti-Goat IgG-FITC
677 (Sigma, F7367). The monoclonal Ab 2B04 was a gift of Ali Ellebedy (Washington
678 University in St. Louis).

bioRxiv preprint doi: https://doi.org/10.1101/2021.06.01.446579; this version posted June 1, 2021. The copyright holder for this preprint (which was not certified by peer review) is the author/funder, who has granted bioRxiv a license to display the preprint in perpetuity. It is made available under aCC-BY-NC 4.0 International license.

679 Inhibitors in this study included Methyl cellulose (Sigma, M0512), Cathepsin L
680 Inhibitor III (Sigma, 219427), CA-074 Me (Sigma, 205531), EST/E-64D (Sigma,
681 330005), Bafilomycin A1 (Sigma, B1793) and Leupeptin (Sigma, L2884). EK1
682 peptide was synthesized by Alpha Diagnostic International (San Antonio, Texas).
683 Patient serum samples were collected from hospitalized COVID-19 patients
684 under The Ohio State University IRB protocol #2020H0228 as described (Zeng et
685 al., 2020). Vaccinee serum samples were collected from health care workers
686 following 3-4 weeks of the second dose of Moderna and Pfizer SARS-CoV-2
687 mRNA vaccination under an amended IRB protocol #2020H0228.

688 **Cell-to-cell transmission**. In the lentiviral vector system, the expression of anti-
689 sense reporter gene Gluc is interrupted by an intron oriented in the sense direction
690 of the HIV-1 genome so that Gluc production will only occur in infected target cells
691 and not virus producer cells (Zeng et al., 2020). By coculturing the virus producer
692 and target cells, cell-to-cell transmission was determined by measuring the Gluc
693 activity of the cocultured media between donor cells (such as 293T) producing
694 lentiviral pseudotypes and target cells (such as 293T/ACE2). Specifically, 293T
695 cells were seeded in 6-well plates and transfected with 1.4 μg NL4.3-inGluc and
696 0.7 μg of plasmids encoding SARS-CoV or SARS-CoV-2 spike. The next day,
697 transfected 293T donor cells were digested with PBS/5 mM EDTA and thoroughly
698 washed with PBS to remove EDTA, followed by coculturing with target cells

bioRxiv preprint doi: https://doi.org/10.1101/2021.06.01.446579; this version posted June 1, 2021. The copyright holder for this preprint (which was not certified by peer review) is the author/funder, who has granted bioRxiv a license to display the preprint in perpetuity. It is made available under aCC-BY-NC 4.0 International license.

699 (293T/ACE2, Caco-2, Calu-3, NCI-H520 or PBMCs) at 1:1 ratio in 24-well plates
700 for 24~72 hr. Inhibitors or sera were added as needed. Supernatants were
701 collected and measured for the Gluc activity.

702 For authentic SARS-CoV-2 WT and VOCs, the donor Vero-ACE2 cells were
703 infected with an MOI of 0.2 (WT) or 0.02 (VOCs) for 20 hr, followed by coculturing
704 with the same number of Vero-mTomato-Red cells for an additional 6 hr, in the
705 presence or absence of vaccinee sera. Cells were then fixed with 3.7%
706 formaldehyde for 1 hr, followed by three times of wash with PBS before being taken
707 out of the BSL3 lab. The fixed cells were incubated with anti-SARS-CoV-2
708 Nucleocapsid and anti-Mouse-FITC, and subjected to flow cytometry analysis.

709 **Cell-free infection.** Cell-free infection was performed along with cell-to-cell
710 transmission in this work. Briefly, an equal number of transfected donor cells were
711 seeded in new 24-well plates and maintained for the same period of time as in cell-
712 to-cell transmission (normally 48-72 hr). The total volumes of supernatants were
713 collected and used to infect target cells, which were seeded with the presence of
714 the same amount of untransfected 293T cells; this would ensure that the total
715 numbers of cells and density used for cell-to-cell and cell-free infection assays
716 were comparable. For the *transwell* setting, the transfected donor cells were
717 seeded onto the insert while target cells, which again were mixed with same
718 amount of untransfected 293T cells, were on the bottom; this would avoid the

bioRxiv preprint doi: https://doi.org/10.1101/2021.06.01.446579; this version posted June 1, 2021. The copyright holder for this preprint (which was not certified by peer review) is the author/funder, who has granted bioRxiv a license to display the preprint in perpetuity. It is made available under aCC-BY-NC 4.0 International license.

719 contact between donor and target cells yet the virus can spread through the filter.
720 Supernatants were collected at the same time points as cell-to-cell transmission
721 and measured for Gluc activity.

722 **Cell-cell fusion**. For fluorescence-based cell-cell fusion, 293T cells were
723 transfected with plasmid encoding GFP and spikes. Following 24 hrs transfection,
724 donor 293T cells were cocultured with target cells. Micrographs of cocultured cells
725 were taken after 2~24 hrs coculture. For tet-off-based assay, 293T cells were
726 transfected with plasmids encoding tet-off or SARS-CoV or SARS-CoV-2 spike
727 and were cocultured with target 293FT-mCAT-Gluc cells (stably expressing
728 tetracycline-responsive element (TRE)-driven *Gaussia* luciferase), which were
729 transfected with a plasmid expressing ACE2; Gluc activity was measured from the
730 supernatant of cocultured cells harvested at 24 and 48 hr, respectively.

731 **Plaque assay.** The replication-competent rVSV-GFP-SARS-CoV and rVSV-GFP-
732 SARS-CoV-2 viruses were used to infect confluent Vero-E6 cells (MOI=0.01) for 1
733 h at 37°C. The uninfected virus was then removed from cells and replaced with
734 1% methylcellulose in DMEM/5% FBS and incubated for 72 hr at 37°C. Cells were
735 fixed with 3.7% paraformaldehyde in PBS and stained with 1% crystal violet
736 (Sigma, C0775) in 10% ethanol for visualization of plaques.

bioRxiv preprint doi: https://doi.org/10.1101/2021.06.01.446579; this version posted June 1, 2021. The copyright holder for this preprint (which was not certified by peer review) is the author/funder, who has granted bioRxiv a license to display the preprint in perpetuity. It is made available under aCC-BY-NC 4.0 International license.

737 **Flow cytometry.** For analysis of spike and ACE2 expression on the cell surface,
738 transfected 293T cells were washed with PBS, detached with PBS/5mM EDTA for
739 10 min, washed twice with cold PBS/2% FBS, and incubated with anti-coronavirus
740 Spike/Nucleocapsid or anti-hACE2 antibody for 1 hr. After three washes with cold
741 PBS/2% FBS, cells were incubated with FITC-conjugated anti-rabbit IgG/anti-
742 mouse IgG or anti-goat IgG (1:200) secondary antibodies for 1 hr. Cells were
743 washed three times with cold PBS /2% FBS and fixed with 3.7% formaldehyde for
744 10 min and analyzed by flow cytometry. For analysis of rVSV-GFP-SARS-CoV and
745 rVSV-GFP-SARS-CoV-2 infection, infected Vero E6 cells were washed with PBS
746 and digested with 0.05% trypsin, followed by fixation with 3.7% formaldehyde for
747 10 min and analyzed by flow cytometry.

748 **Western blotting.** Western blotting was performed as previously described (Li et
749 al., 2019; Zeng et al., 2020). In brief, HEK293T cells were collected and lysed in
750 RIPA buffer (50 mM Tris, pH 7.5, 150 mM NaCl, 1 mM EDTA, 1% Nonidet P-40,
751 0.1% SDS, protease inhibitor cocktail) for 40 min on ice, followed by centrifugation
752 for 10 min, 12,000 x g at 4°C, Cell lysate then boiled at 100 ℃ for 10 min with
753 1XSDS loading buffer containing 2-Mercaptoethanol. Samples were run on 10%
754 SDS-PAGE gels, transferred to PVDF membranes, and probed with primary
755 antibodies and secondary antibodies, analyzed by Amersham Imager 600
756 (Thermofisher).

bioRxiv preprint doi: https://doi.org/10.1101/2021.06.01.446579; this version posted June 1, 2021. The copyright holder for this preprint (which was not certified by peer review) is the author/funder, who has granted bioRxiv a license to display the preprint in perpetuity. It is made available under aCC-BY-NC 4.0 International license.

757 **Neutralization assays.** Cell-free virus neutralization assays were performed by
758 incubating free virus with serial diluted Moderna and Pfizer vaccinee sera, followed
759 by infecting 293T/ACE2 target cells and measuring the luciferase activity (Zeng et
760 al., 2020) at 48 and 72 hr. Cell-to-cell virus neutralization assays were performed
761 by incubating serial diluted sera with viral producer cells (transfected 293T) and
762 target cells (293T/ACE2) in the coculture system, and supernatants were collected
763 at 48 and 72 hr to measure the luciferase activity. In both cases, NT_{50} was defined
764 as the sera dilution fold at which the relative light units were reduced by 50%
765 compared with the control wells (no sera); the NT_{50} values were calculated using
766 nonlinear regression in GraphPad Prism.

767 **QUANTIFICATION AND STATISTICAL ANALYSIS**

768 **Statistical Analysis**

769 Data were analyzed as mean with Standard Error of Mean (SEM). All experiments
770 were performed at least three independent replications, and the number of
771 biological replicates for each data set is given by “n” and is provided in the
772 respective figure legend. Statistical analyses were performed using GraphPad
773 Prism 5.0 as follows: One-way Analysis of Variance (ANOVA) with Bonferroni’s
774 post-tests was used to compute statistical significance between multiple groups
775 for multiple comparison or t-test was used for two groups for single comparison. A

bioRxiv preprint doi: https://doi.org/10.1101/2021.06.01.446579; this version posted June 1, 2021. The copyright holder for this preprint (which was not certified by peer review) is the author/funder, who has granted bioRxiv a license to display the preprint in perpetuity. It is made available under aCC-BY-NC 4.0 International license.

776 p value of less than 0.05 was considered significant and indicated by an asterisk
777 (*, p<0.05).
778
779 **Supplemental Figures**
780 **Figure S1. Effects of methylcellulose and monoclonal antibody 2B04 on**
781 **rVSV-GFP transmission in Vero-E6 cells.** Vero-E6 cells were infected with
782 appropriate MOIs of either VSV-GFP-SARS-CoV or VSV-GFP-SARS-CoV-2. After
783 16 h post-infection, the infected Vero-E6 cells were cocultured with Vero-
784 mTomato-Red cells at 1:1 ratio, in the presence or absence of 2 μg/mL 2B04 or 1%
785 methylcellulose. Micrographs of cocultured cells were taken after 18 h coculture
786 **(A and D)**, with dual fluorescence positive cells indicated by arrows. The GFP
787 signals in Tomato-positive cells were analyzed by flow cytometry **(B and E**, Q2**)**,
788 indicative of virus transmission from Vero-E6 to Vero-mTomato-Red cells. Results
789 from 3 independent experiment (n=3) were summarized and plotted as relative
790 infection rates by setting the values of mock infection control to 1.0 (**C and F**).
791
792 **Figure S2. Role of ACE2 in cell-to-cell transmission. (A and B)** The expression
793 level of ACE2 in target cells was analyzed by flow cytometry **(A)** and western
794 blotting **(B)** using a specific antibody against ACE2; results were one
795 representative of three independent experiments. **(C)** Representative images of
796 cell-cell fusion induced by SARS-CoV-2 and SARS-CoV spike at indicated doses

bioRxiv preprint doi: https://doi.org/10.1101/2021.06.01.446579; this version posted June 1, 2021. The copyright holder for this preprint (which was not certified by peer review) is the author/funder, who has granted bioRxiv a license to display the preprint in perpetuity. It is made available under aCC-BY-NC 4.0 International license.

797 of ACE2. **(D)** The expression level of ACE2 in different cell lines and human
798 PBMCs. qPCR was performed to quantify the ACE2 mRNA expression and relative
799 expression was plotted by setting the value of 293T cells to 1.0. ND: not detected.
800 **(E and F)** Cell-to-cell transmission in Calu-3 cells. Experiments were performed as
801 described in Figures 1 and 4, except that Calu-3 cells were used as target cells,
802 which were cocultured with viral producer 293T cells (n=3).
803
804 **Figure S3. Effect of endosomal entry inhibitors on cell-cell fusion induced by**
805 **SARS-CoV-2 spike**. Experiments were carried out as described in Figures 3 and
806 5, with indicated inhibitors included in the cell coculture: 5 μM Cat L inhibitor III, 5
807 μM CA-074, 30 μM E-64D, 50 nM BafA1, and 50 μM leupeptin.
808
809 **Figure S4. Neutralization curves of vaccinee sera against the cell-to-cell and**
810 **cell-free infection of VOCs B1.1.7 and B.1.351 relative to D614G and WT. (A)**
811 Flow cytometric gating control in analysis of data presented in Figure 7A using
812 uninfected Vero-ACE2 and Vero-mTomato-Red cells. **(B and C)** Six vaccinee sera
813 samples, 3 from Moderna and 3 from Pfizer, were chosen for the neutralization
814 assay in the context of cell-to-cell transmission or cell-free infection. The y axis
815 indicates the relative viral infectivity by setting the viral infectivity without serum to
816 100%; the x axis indicates dilution fold of serum samples (n=6).
817

bioRxiv preprint doi: https://doi.org/10.1101/2021.06.01.446579; this version posted June 1, 2021. The copyright holder for this preprint (which was not certified by peer review) is the author/funder, who has granted bioRxiv a license to display the preprint in perpetuity. It is made available under aCC-BY-NC 4.0 International license.

818 **REFERENCES**

819 Acharya, D., Liu, G., and Gack, M.U. (2020). Dysregulation of type I interferon responses
820 in COVID-19. Nat Rev Immunol *20*, 397-398.
821 Agosto, L.M., Zhong, P., Munro, J., and Mothes, W. (2014). Highly active antiretroviral
822 therapies are effective against HIV-1 cell-to-cell transmission. PLoS Pathog *10*, e1003982.
823 Alpert, T., Brito, A.F., Lasek-Nesselquist, E., Rothman, J., Valesano, A.L., MacKay, M.J.,
824 Petrone, M.E., Breban, M.I., Watkins, A.E., Vogels, C.B.F.*, et al.* (2021). Early introductions
825 and transmission of SARS-CoV-2 variant B.1.1.7 in the United States. Cell *184*, 2595-
826 2604 e2513.
827 Alsoussi, W.B., Turner, J.S., Case, J.B., Zhao, H., Schmitz, A.J., Zhou, J.Q., Chen, R.E.,
828 Lei, T., Rizk, A.A., McIntire, K.M.*, et al.* (2020). A Potently Neutralizing Antibody Protects
829 Mice against SARS-CoV-2 Infection. J Immunol *205*, 915-922.
830 Banerjee, A., Nasir, J.A., Budylowski, P., Yip, L., Aftanas, P., Christie, N., Ghalami, A., Baid,
831 K., Raphenya, A.R., Hirota, J.A.*, et al.* (2020). Isolation, Sequence, Infectivity, and
832 Replication Kinetics of Severe Acute Respiratory Syndrome Coronavirus 2. Emerging
833 infectious diseases *26*, 2054-2063.
834 Barnes, C.O., Jette, C.A., Abernathy, M.E., Dam, K.A., Esswein, S.R., Gristick, H.B.,
835 Malyutin, A.G., Sharaf, N.G., Huey-Tubman, K.E., Lee, Y.E.*, et al.* (2020). SARS-CoV-2
836 neutralizing antibody structures inform therapeutic strategies. Nature *588*, 682-687.
837 Baum, A., Fulton, B.O., Wloga, E., Copin, R., Pascal, K.E., Russo, V., Giordano, S., Lanza,
838 K., Negron, N., Ni, M.*, et al.* (2020). Antibody cocktail to SARS-CoV-2 spike protein

bioRxiv preprint doi: https://doi.org/10.1101/2021.06.01.446579; this version posted June 1, 2021. The copyright holder for this preprint (which was not certified by peer review) is the author/funder, who has granted bioRxiv a license to display the preprint in perpetuity. It is made available under aCC-BY-NC 4.0 International license.

839 prevents rapid mutational escape seen with individual antibodies. Science *369*, 1014-1018.
840 Brimacombe, C.L., Grove, J., Meredith, L.W., Hu, K., Syder, A.J., Flores, M.V., Timpe, J.M.,
841 Krieger, S.E., Baumert, T.F., Tellinghuisen, T.L.*, et al.* (2011). Neutralizing antibody-
842 resistant hepatitis C virus cell-to-cell transmission. J Virol *85*, 596-605.
843 Brooke, G.N., and Prischi, F. (2020). Structural and functional modelling of SARS-CoV-2
844 entry in animal models. Scientific reports *10*, 15917.
845 Carrington, J.C., Kasschau, K.D., Mahajan, S.K., and Schaad, M.C. (1996). Cell-to-Cell
846 and Long-Distance Transport of Viruses in Plants. The Plant cell *8*, 1669-1681.
847 Carvalho, T., Krammer, F., and Iwasaki, A. (2021). The first 12 months of COVID-19: a
848 timeline of immunological insights. Nat Rev Immunol *21*, 245-256.
849 Case, J.B., Rothlauf, P.W., Chen, R.E., Liu, Z., Zhao, H., Kim, A.S., Bloyet, L.M., Zeng, Q.,
850 Tahan, S., Droit, L.*, et al.* (2020). Neutralizing Antibody and Soluble ACE2 Inhibition of a
851 Replication-Competent VSV-SARS-CoV-2 and a Clinical Isolate of SARS-CoV-2. Cell
852 Host Microbe *28*, 475-485 e475.
853 Chan, J.F., Kok, K.H., Zhu, Z., Chu, H., To, K.K., Yuan, S., and Yuen, K.Y. (2020). Genomic
854 characterization of the 2019 novel human-pathogenic coronavirus isolated from a patient
855 with atypical pneumonia after visiting Wuhan. Emerg Microbes Infect *9*, 221-236.
856 Chu, H., Chan, J.F., Wang, Y., Yuen, T.T., Chai, Y., Hou, Y., Shuai, H., Yang, D., Hu, B.,
857 Huang, X.*, et al.* (2020). Comparative Replication and Immune Activation Profiles of
858 SARS-CoV-2 and SARS-CoV in Human Lungs: An Ex Vivo Study With Implications for the
859 Pathogenesis of COVID-19. Clinical infectious diseases : an official publication of the

bioRxiv preprint doi: https://doi.org/10.1101/2021.06.01.446579; this version posted June 1, 2021. The copyright holder for this preprint (which was not certified by peer review) is the author/funder, who has granted bioRxiv a license to display the preprint in perpetuity. It is made available under aCC-BY-NC 4.0 International license.

860 Infectious Diseases Society of America *71*, 1400-1409.

861 Chu, H., Hu, B., Huang, X., Chai, Y., Zhou, D., Wang, Y., Shuai, H., Yang, D., Hou, Y.,

862 Zhang, X.*, et al.* (2021). Host and viral determinants for efficient SARS-CoV-2 infection of

863 the human lung. Nat Commun *12*, 134.

864 Cifuentes-Munoz, N., Dutch, R.E., and Cattaneo, R. (2018). Direct cell-to-cell transmission

865 of respiratory viruses: The fast lanes. PLoS Pathog *14*, e1007015.

866 Coutard, B., Valle, C., de Lamballerie, X., Canard, B., Seidah, N.G., and Decroly, E. (2020).

867 The spike glycoprotein of the new coronavirus 2019-nCoV contains a furin-like cleavage

868 site absent in CoV of the same clade. Antiviral Res *176*, 104742.

869 Dale, B.M., Alvarez, R.A., and Chen, B.K. (2013). Mechanisms of enhanced HIV spread

870 through T-cell virological synapses. Immunological reviews *251*, 113-124.

871 Dale, B.M., McNerney, G.P., Thompson, D.L., Hubner, W., de Los Reyes, K., Chuang, F.Y.,

872 Huser, T., and Chen, B.K. (2011). Cell-to-cell transfer of HIV-1 via virological synapses

873 leads to endosomal virion maturation that activates viral membrane fusion. Cell Host

874 Microbe *10*, 551-562.

875 Dispinseri, S., Secchi, M., Pirillo, M.F., Tolazzi, M., Borghi, M., Brigatti, C., De Angelis, M.L.,

876 Baratella, M., Bazzigaluppi, E., Venturi, G.*, et al.* (2021). Neutralizing antibody responses

877 to SARS-CoV-2 in symptomatic COVID-19 is persistent and critical for survival. Nat

878 Commun *12*, 2670.

879 Duan, L., Zheng, Q., Zhang, H., Niu, Y., Lou, Y., and Wang, H. (2020). The SARS-CoV-2

880 Spike Glycoprotein Biosynthesis, Structure, Function, and Antigenicity: Implications for the

bioRxiv preprint doi: https://doi.org/10.1101/2021.06.01.446579; this version posted June 1, 2021. The copyright holder for this preprint (which was not certified by peer review) is the author/funder, who has granted bioRxiv a license to display the preprint in perpetuity. It is made available under aCC-BY-NC 4.0 International license.

881 Design of Spike-Based Vaccine Immunogens. Frontiers in immunology *11*, 576622.
882 Funk, T., Pharris, A., Spiteri, G., Bundle, N., Melidou, A., Carr, M., Gonzalez, G., Garcia-
883 Leon, A., Crispie, F., O'Connor, L.*, et al.* (2021). Characteristics of SARS-CoV-2 variants
884 of concern B.1.1.7, B.1.351 or P.1: data from seven EU/EEA countries, weeks 38/2020 to
885 10/2021. Euro surveillance : bulletin Europeen sur les maladies transmissibles =
886 European communicable disease bulletin *26*.
887 Grubaugh, N.D., Hodcroft, E.B., Fauver, J.R., Phelan, A.L., and Cevik, M. (2021). Public
888 health actions to control new SARS-CoV-2 variants. Cell *184*, 1127-1132.
889 Harrison, A.G., Lin, T., and Wang, P. (2020). Mechanisms of SARS-CoV-2 Transmission
890 and Pathogenesis. Trends Immunol *41*, 1100-1115.
891 Hipper, C., Brault, V., Ziegler-Graff, V., and Revers, F. (2013). Viral and cellular factors
892 involved in Phloem transport of plant viruses. Frontiers in plant science *4*, 154.
893 Hoffmann, M., Kleine-Weber, H., Schroeder, S., Kruger, N., Herrler, T., Erichsen, S.,
894 Schiergens, T.S., Herrler, G., Wu, N.H., Nitsche, A.*, et al.* (2020). SARS-CoV-2 Cell Entry
895 Depends on ACE2 and TMPRSS2 and Is Blocked by a Clinically Proven Protease Inhibitor.
896 Cell *181*, 271-280 e278.
897 Huang, Y., Yang, C., Xu, X.F., Xu, W., and Liu, S.W. (2020). Structural and functional
898 properties of SARS-CoV-2 spike protein: potential antivirus drug development for COVID-
899 19. Acta pharmacologica Sinica *41*, 1141-1149.
900 Hui, K.P.Y., Cheung, M.C., Perera, R., Ng, K.C., Bui, C.H.T., Ho, J.C.W., Ng, M.M.T., Kuok,
901 D.I.T., Shih, K.C., Tsao, S.W.*, et al.* (2020). Tropism, replication competence, and innate

bioRxiv preprint doi: https://doi.org/10.1101/2021.06.01.446579; this version posted June 1, 2021. The copyright holder for this preprint (which was not certified by peer review) is the author/funder, who has granted bioRxiv a license to display the preprint in perpetuity. It is made available under aCC-BY-NC 4.0 International license.

902 immune responses of the coronavirus SARS-CoV-2 in human respiratory tract and
903 conjunctiva: an analysis in ex-vivo and in-vitro cultures. The Lancet Respiratory medicine
904 *8*, 687-695.
905 Jeyanathan, M., Afkhami, S., Smaill, F., Miller, M.S., Lichty, B.D., and Xing, Z. (2020).
906 Immunological considerations for COVID-19 vaccine strategies. Nat Rev Immunol *20*,
907 615-632.
908 Khan, A., Zia, T., Suleman, M., Khan, T., Ali, S.S., Abbasi, A.A., Mohammad, A., and Wei,
909 D.Q. (2021). Higher infectivity of the SARS-CoV-2 new variants is associated with
910 K417N/T, E484K, and N501Y mutants: An insight from structural data. Journal of cellular
911 physiology.
912 Kissler, S.M., Fauver, J.R., Mack, C., Tai, C.G., Breban, M.I., Watkins, A.E., Samant, R.M.,
913 Anderson, D.J., Ho, D.D., Grubaugh, N.D.*, et al.* (2021). Densely sampled viral trajectories
914 suggest longer duration of acute infection with B.1.1.7 variant relative to non-B.1.1.7
915 SARS-CoV-2. medRxiv, 2021.2002.2016.21251535.
916 Lan, J., Ge, J., Yu, J., Shan, S., Zhou, H., Fan, S., Zhang, Q., Shi, X., Wang, Q., Zhang,
917 L.*, et al.* (2020). Structure of the SARS-CoV-2 spike receptor-binding domain bound to the
918 ACE2 receptor. Nature *581*, 215-220.
919 Law, K.M., Satija, N., Esposito, A.M., and Chen, B.K. (2016). Cell-to-Cell Spread of HIV
920 and Viral Pathogenesis. Adv Virus Res *95*, 43-85.
921 Li, F. (2016). Structure, Function, and Evolution of Coronavirus Spike Proteins. Annu Rev
922 Virol *3*, 237-261.

bioRxiv preprint doi: https://doi.org/10.1101/2021.06.01.446579; this version posted June 1, 2021. The copyright holder for this preprint (which was not certified by peer review) is the author/funder, who has granted bioRxiv a license to display the preprint in perpetuity. It is made available under aCC-BY-NC 4.0 International license.

923 Li, H., Zony, C., Chen, P., and Chen, B.K. (2017). Reduced Potency and Incomplete
924 Neutralization of Broadly Neutralizing Antibodies against Cell-to-Cell Transmission of HIV-
925 1 with Transmitted Founder Envs. J Virol *91*.
926 Li, M., Waheed, A.A., Yu, J., Zeng, C., Chen, H.Y., Zheng, Y.M., Feizpour, A., Reinhard,
927 B.M., Gummuluru, S., Lin, S.*, et al.* (2019). TIM-mediated inhibition of HIV-1 release is
928 antagonized by Nef but potentiated by SERINC proteins. Proc Natl Acad Sci U S A *116*,
929 5705-5714.
930 Lowery, S.A., Sariol, A., and Perlman, S. (2021). Innate immune and inflammatory
931 responses to SARS-CoV-2: Implications for COVID-19. Cell Host Microbe.
932 Lukassen, S., Chua, R.L., Trefzer, T., Kahn, N.C., Schneider, M.A., Muley, T., Winter, H.,
933 Meister, M., Veith, C., Boots, A.W.*, et al.* (2020). SARS-CoV-2 receptor ACE2 and
934 TMPRSS2 are primarily expressed in bronchial transient secretory cells. EMBO J *39*,
935 e105114.
936 Markosyan, R.M., Miao, C., Zheng, Y.M., Melikyan, G.B., Liu, S.L., and Cohen, F.S. (2016).
937 Induction of Cell-Cell Fusion by Ebola Virus Glycoprotein: Low pH Is Not a Trigger. PLoS
938 Pathog *12*, e1005373.
939 Mazurov, D., Ilinskaya, A., Heidecker, G., Lloyd, P., and Derse, D. (2010). Quantitative
940 comparison of HTLV-1 and HIV-1 cell-to-cell infection with new replication dependent
941 vectors. PLoS Pathog *6*, e1000788.
942 Miao, C., Li, M., Zheng, Y.M., Cohen, F.S., and Liu, S.L. (2016). Cell-cell contact promotes
943 Ebola virus GP-mediated infection. Virology *488*, 202-215.

bioRxiv preprint doi: https://doi.org/10.1101/2021.06.01.446579; this version posted June 1, 2021. The copyright holder for this preprint (which was not certified by peer review) is the author/funder, who has granted bioRxiv a license to display the preprint in perpetuity. It is made available under aCC-BY-NC 4.0 International license.

944 Mothes, W., Sherer, N.M., Jin, J., and Zhong, P. (2010). Virus cell-to-cell transmission. J
945 Virol *84*, 8360-8368.
946 Murgolo, N., Therien, A.G., Howell, B., Klein, D., Koeplinger, K., Lieberman, L.A., Adam,
947 G.C., Flynn, J., McKenna, P., Swaminathan, G.*, et al.* (2021). SARS-CoV-2 tropism, entry,
948 replication, and propagation: Considerations for drug discovery and development. PLoS
949 Pathog *17*, e1009225.
950 Nitulescu, G.M., Paunescu, H., Moschos, S.A., Petrakis, D., Nitulescu, G., Ion, G.N.D.,
951 Spandidos, D.A., Nikolouzakis, T.K., Drakoulis, N., and Tsatsakis, A. (2020).
952 Comprehensive analysis of drugs to treat SARSCoV2 infection: Mechanistic insights into
953 current COVID19 therapies (Review). International journal of molecular medicine *46*, 467-
954 488.
955 Noh, J.Y., Jeong, H.W., and Shin, E.C. (2021). SARS-CoV-2 mutations, vaccines, and
956 immunity: implication of variants of concern. Signal Transduct Target Ther *6*, 203.
957 Ou, X., Liu, Y., Lei, X., Li, P., Mi, D., Ren, L., Guo, L., Guo, R., Chen, T., Hu, J.*, et al.* (2020).
958 Characterization of spike glycoprotein of SARS-CoV-2 on virus entry and its immune
959 cross-reactivity with SARS-CoV. Nat Commun *11*, 1620.
960 Park, A., and Iwasaki, A. (2020). Type I and Type III Interferons - Induction, Signaling,
961 Evasion, and Application to Combat COVID-19. Cell Host Microbe *27*, 870-878.
962 Planas, D., Bruel, T., Grzelak, L., Guivel-Benhassine, F., Staropoli, I., Porrot, F., Planchais,
963 C., Buchrieser, J., Rajah, M.M., Bishop, E.*, et al.* (2021). Sensitivity of infectious SARS-
964 CoV-2 B.1.1.7 and B.1.351 variants to neutralizing antibodies. Nature medicine *27*, 917-

bioRxiv preprint doi: https://doi.org/10.1101/2021.06.01.446579; this version posted June 1, 2021. The copyright holder for this preprint (which was not certified by peer review) is the author/funder, who has granted bioRxiv a license to display the preprint in perpetuity. It is made available under aCC-BY-NC 4.0 International license.

965 924.

966 Plante, J.A., Liu, Y., Liu, J., Xia, H., Johnson, B.A., Lokugamage, K.G., Zhang, X., Muruato,
967 A.E., Zou, J., Fontes-Garfias, C.R., *et al.* (2021). Spike mutation D614G alters SARS-
968 CoV-2 fitness. Nature *592*, 116-121.

969 Roback, J.D., and Guarner, J. (2020). Convalescent Plasma to Treat COVID-19:
970 Possibilities and Challenges. Jama *323*, 1561-1562.

971 Rogers, T.F., Zhao, F., Huang, D., Beutler, N., Burns, A., He, W.T., Limbo, O., Smith, C.,
972 Song, G., Woehl, J., *et al.* (2020). Isolation of potent SARS-CoV-2 neutralizing antibodies
973 and protection from disease in a small animal model. Science *369*, 956-963.

974 Sattentau, Q. (2008). Avoiding the void: cell-to-cell spread of human viruses. Nature
975 reviews Microbiology *6*, 815-826.

976 Shang, J., Wan, Y., Luo, C., Ye, G., Geng, Q., Auerbach, A., and Li, F. (2020). Cell entry
977 mechanisms of SARS-CoV-2. Proc Natl Acad Sci U S A *117*, 11727-11734.

978 Stewart-Jones, G.B., Soto, C., Lemmin, T., Chuang, G.Y., Druz, A., Kong, R., Thomas,
979 P.V., Wagh, K., Zhou, T., Behrens, A.J., *et al.* (2016). Trimeric HIV-1-Env Structures Define
980 Glycan Shields from Clades A, B, and G. Cell *165*, 813-826.

981 Sun, Z., Ren, K., Zhang, X., Chen, J., Jiang, Z., Jiang, J., Ji, F., Ouyang, X., and Li, L.
982 (2020). Mass Spectrometry Analysis of Newly Emerging Coronavirus HCoV-19 Spike
983 Protein and Human ACE2 Reveals Camouflaging Glycans and Unique Post-Translational
984 Modifications. Engineering.

985 Titanji, B.K., Aasa-Chapman, M., Pillay, D., and Jolly, C. (2013). Protease inhibitors

bioRxiv preprint doi: https://doi.org/10.1101/2021.06.01.446579; this version posted June 1, 2021. The copyright holder for this preprint (which was not certified by peer review) is the author/funder, who has granted bioRxiv a license to display the preprint in perpetuity. It is made available under aCC-BY-NC 4.0 International license.

986 effectively block cell-to-cell spread of HIV-1 between T cells. Retrovirology *10*, 161.

987 V'Kovski, P., Kratzel, A., Steiner, S., Stalder, H., and Thiel, V. (2021). Coronavirus biology
988 and replication: implications for SARS-CoV-2. Nature reviews Microbiology *19*, 155-170.

989 Walensky, R.P., Walke, H.T., and Fauci, A.S. (2021). SARS-CoV-2 Variants of Concern in
990 the United States-Challenges and Opportunities. Jama *325*, 1037-1038.

991 Walls, A.C., Park, Y.J., Tortorici, M.A., Wall, A., McGuire, A.T., and Veesler, D. (2020).
992 Structure, Function, and Antigenicity of the SARS-CoV-2 Spike Glycoprotein. Cell *181*,
993 281-292 e286.

994 Wang, L., Eng, E.T., Law, K., Gordon, R.E., Rice, W.J., and Chen, B.K. (2017).
995 Visualization of HIV T Cell Virological Synapses and Virus-Containing Compartments by
996 Three-Dimensional Correlative Light and Electron Microscopy. J Virol *91*.

997 Wang, P., Nair, M.S., Liu, L., Iketani, S., Luo, Y., Guo, Y., Wang, M., Yu, J., Zhang, B.,
998 Kwong, P.D., *et al.* (2021). Antibody resistance of SARS-CoV-2 variants B.1.351 and
999 B.1.1.7. Nature *593*, 130-135.

1000 Wang, Q., Zhang, Y., Wu, L., Niu, S., Song, C., Zhang, Z., Lu, G., Qiao, C., Hu, Y., Yuen,
1001 K.Y., *et al.* (2020). Structural and Functional Basis of SARS-CoV-2 Entry by Using Human
1002 ACE2. Cell *181*, 894-904 e899.

1003 Watanabe, Y., Berndsen, Z.T., Raghwani, J., Seabright, G.E., Allen, J.D., Pybus, O.G.,
1004 McLellan, J.S., Wilson, I.A., Bowden, T.A., Ward, A.B., *et al.* (2020). Vulnerabilities in
1005 coronavirus glycan shields despite extensive glycosylation. Nat Commun *11*, 2688.

1006 White, J.M., Delos, S.E., Brecher, M., and Schornberg, K. (2008). Structures and

bioRxiv preprint doi: https://doi.org/10.1101/2021.06.01.446579; this version posted June 1, 2021. The copyright holder for this preprint (which was not certified by peer review) is the author/funder, who has granted bioRxiv a license to display the preprint in perpetuity. It is made available under aCC-BY-NC 4.0 International license.

1007 mechanisms of viral membrane fusion proteins: multiple variations on a common theme.
1008 Crit Rev Biochem Mol Biol *43*, 189-219.
1009 Wrapp, D., Wang, N., Corbett, K.S., Goldsmith, J.A., Hsieh, C.L., Abiona, O., Graham,
1010 B.S., and McLellan, J.S. (2020). Cryo-EM structure of the 2019-nCoV spike in the
1011 prefusion conformation. Science *367*, 1260-1263.
1012 Wu, A., Wang, L., Zhou, H.Y., Ji, C.Y., Xia, S.Z., Cao, Y., Meng, J., Ding, X., Gold, S., Jiang,
1013 T., *et al.* (2021). One year of SARS-CoV-2 evolution. Cell Host Microbe *29*, 503-507.
1014 Xia, S., Yan, L., Xu, W., Agrawal, A.S., Algaissi, A., Tseng, C.K., Wang, Q., Du, L., Tan, W.,
1015 Wilson, I.A., *et al.* (2019). A pan-coronavirus fusion inhibitor targeting the HR1 domain of
1016 human coronavirus spike. Sci Adv *5*, eaav4580.
1017 Xia, S., Zhu, Y., Liu, M., Lan, Q., Xu, W., Wu, Y., Ying, T., Liu, S., Shi, Z., Jiang, S., *et al.*
1018 (2020). Fusion mechanism of 2019-nCoV and fusion inhibitors targeting HR1 domain in
1019 spike protein. Cell Mol Immunol *17*, 765-767.
1020 Xiao, F., Fofana, I., Heydmann, L., Barth, H., Soulier, E., Habersetzer, F., Doffoel, M., Bukh,
1021 J., Patel, A.H., Zeisel, M.B., *et al.* (2014). Hepatitis C virus cell-cell transmission and
1022 resistance to direct-acting antiviral agents. PLoS Pathog *10*, e1004128.
1023 Xie, X., Liu, Y., Liu, J., Zhang, X., Zou, J., Fontes-Garfias, C.R., Xia, H., Swanson, K.A.,
1024 Cutler, M., Cooper, D., *et al.* (2021). Neutralization of SARS-CoV-2 spike 69/70 deletion,
1025 E484K and N501Y variants by BNT162b2 vaccine-elicited sera. Nature medicine *27*, 620-
1026 621.
1027 Yang, D., Chu, H., Hou, Y., Chai, Y., Shuai, H., Lee, A.C., Zhang, X., Wang, Y., Hu, B.,

bioRxiv preprint doi: https://doi.org/10.1101/2021.06.01.446579; this version posted June 1, 2021. The copyright holder for this preprint (which was not certified by peer review) is the author/funder, who has granted bioRxiv a license to display the preprint in perpetuity. It is made available under aCC-BY-NC 4.0 International license.

1028 Huang, X., *et al.* (2020). Attenuated Interferon and Proinflammatory Response in SARS-
1029 CoV-2-Infected Human Dendritic Cells Is Associated With Viral Antagonism of STAT1
1030 Phosphorylation. The Journal of infectious diseases *222*, 734-745.

1031 Yeung, M.L., Teng, J.L.L., Jia, L., Zhang, C., Huang, C., Cai, J.P., Zhou, R., Chan, K.H.,
1032 Zhao, H., Zhu, L., *et al.* (2021). Soluble ACE2-mediated cell entry of SARS-CoV-2 via
1033 interaction with proteins related to the renin-angiotensin system. Cell *184*, 2212-2228
1034 e2212.

1035 Zeng, C., Evans, J.P., Pearson, R., Qu, P., Zheng, Y.M., Robinson, R.T., Hall-Stoodley, L.,
1036 Yount, J., Pannu, S., Mallampalli, R.K., *et al.* (2020). Neutralizing antibody against SARS-
1037 CoV-2 spike in COVID-19 patients, health care workers, and convalescent plasma donors.
1038 JCI Insight *5*.

1039 Zhang, L., Jackson, C.B., Mou, H., Ojha, A., Peng, H., Quinlan, B.D., Rangarajan, E.S.,
1040 Pan, A., Vanderheiden, A., Suthar, M.S., *et al.* (2020a). SARS-CoV-2 spike-protein D614G
1041 mutation increases virion spike density and infectivity. Nat Commun *11*, 6013.

1042 Zhang, Q., Bastard, P., Liu, Z., Le Pen, J., Moncada-Velez, M., Chen, J., Ogishi, M., Sabli,
1043 I.K.D., Hodeib, S., Korol, C., *et al.* (2020b). Inborn errors of type I IFN immunity in patients
1044 with life-threatening COVID-19. Science *370*.

1045 Zhong, P., Agosto, L.M., Ilinskaya, A., Dorjbal, B., Truong, R., Derse, D., Uchil, P.D.,
1046 Heidecker, G., and Mothes, W. (2013a). Cell-to-cell transmission can overcome multiple
1047 donor and target cell barriers imposed on cell-free HIV. PLoS One *8*, e53138.

1048 Zhong, P., Agosto, L.M., Munro, J.B., and Mothes, W. (2013b). Cell-to-cell transmission of

bioRxiv preprint doi: https://doi.org/10.1101/2021.06.01.446579; this version posted June 1, 2021. The copyright holder for this preprint (which was not certified by peer review) is the author/funder, who has granted bioRxiv a license to display the preprint in perpetuity. It is made available under aCC-BY-NC 4.0 International license.

1049 viruses. Current opinion in virology *3*, 44-50.

1050 Zhou, B., Thao, T.T.N., Hoffmann, D., Taddeo, A., Ebert, N., Labroussaa, F., Pohlmann, A.,
1051 King, J., Steiner, S., Kelly, J.N., *et al.* (2021). SARS-CoV-2 spike D614G change enhances
1052 replication and transmission. Nature *592*, 122-127.

1053 Zhou, F., Yu, T., Du, R., Fan, G., Liu, Y., Liu, Z., Xiang, J., Wang, Y., Song, B., Gu, X., *et*
1054 *al.* (2020a). Clinical course and risk factors for mortality of adult inpatients with COVID-19
1055 in Wuhan, China: a retrospective cohort study. Lancet *395*, 1054-1062.

1056 Zhou, P., Yang, X.L., Wang, X.G., Hu, B., Zhang, L., Zhang, W., Si, H.R., Zhu, Y., Li, B.,
1057 Huang, C.L., *et al.* (2020b). A pneumonia outbreak associated with a new coronavirus of
1058 probable bat origin. Nature *579*, 270-273.

1059 Zost, S.J., Gilchuk, P., Case, J.B., Binshtein, E., Chen, R.E., Nkolola, J.P., Schafer, A.,
1060 Reidy, J.X., Trivette, A., Nargi, R.S., *et al.* (2020). Potently neutralizing and protective
1061 human antibodies against SARS-CoV-2. Nature *584*, 443-449.

1062

1063 **Highlights**

1064 *1. SARS-CoV-2 spike efficiently mediates cell-to-cell transmission*
1065 *2. Cell-cell fusion promotes cell-to-cell transmission of SARS-CoV-2*
1066 *3. ACE2 enhances but is not essential for cell-to-cell transmission*
1067 4. *Cell-to-cell transmission of SARS-CoV-2 is resistant to Ab neutralization*

1068 **In Brief**

1069 *The spike protein of SARS-CoV-2 mediates cell-to-cell transmission that is*
1070 *promoted by cell-cell fusion. ACE2 enhances cell-to-cell transmission but is not*
1071 *essential. Cell-to-cell transmission of SARS-CoV-2 is refractory to antibody*
1072 *neutralization.*

1073

was not certified by peer review) is the author/funder, who has granted bioRxiv a license to display the preprint in perpetuity. It is made
available under aCC-BY-NC 4.0 International license.

Graphical Abstract

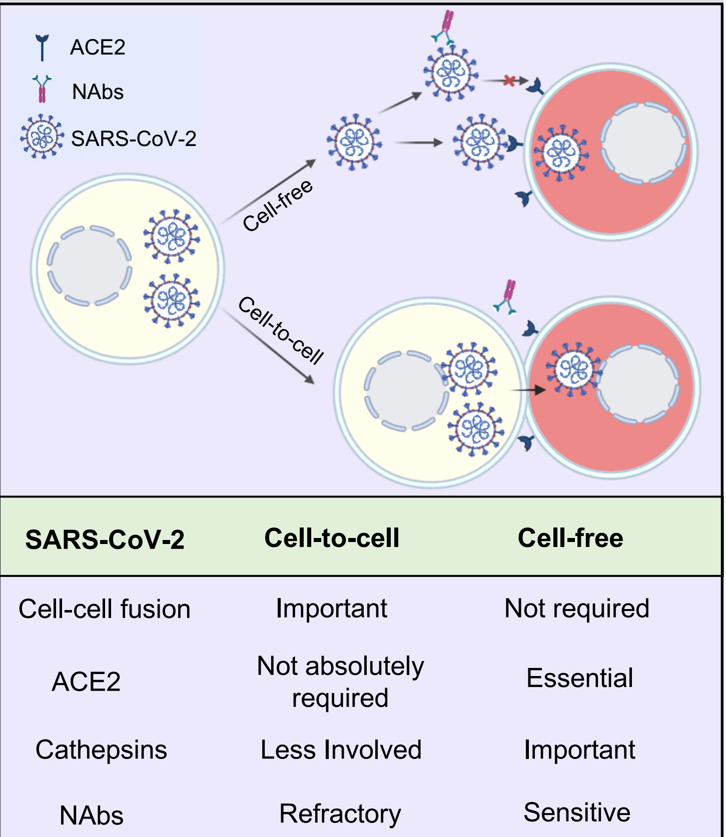

SARS-CoV-2	Cell-to-cell	Cell-free
Cell-cell fusion	Important	Not required
ACE2	Not absolutely required	Essential
Cathepsins	Less Involved	Important
NAbs	Refractory	Sensitive

was not certified by peer review) is the author/funder, who has granted bioRxiv a license to display the preprint in perpetuity. It is made available under aCC-BY-NC 4.0 International license.

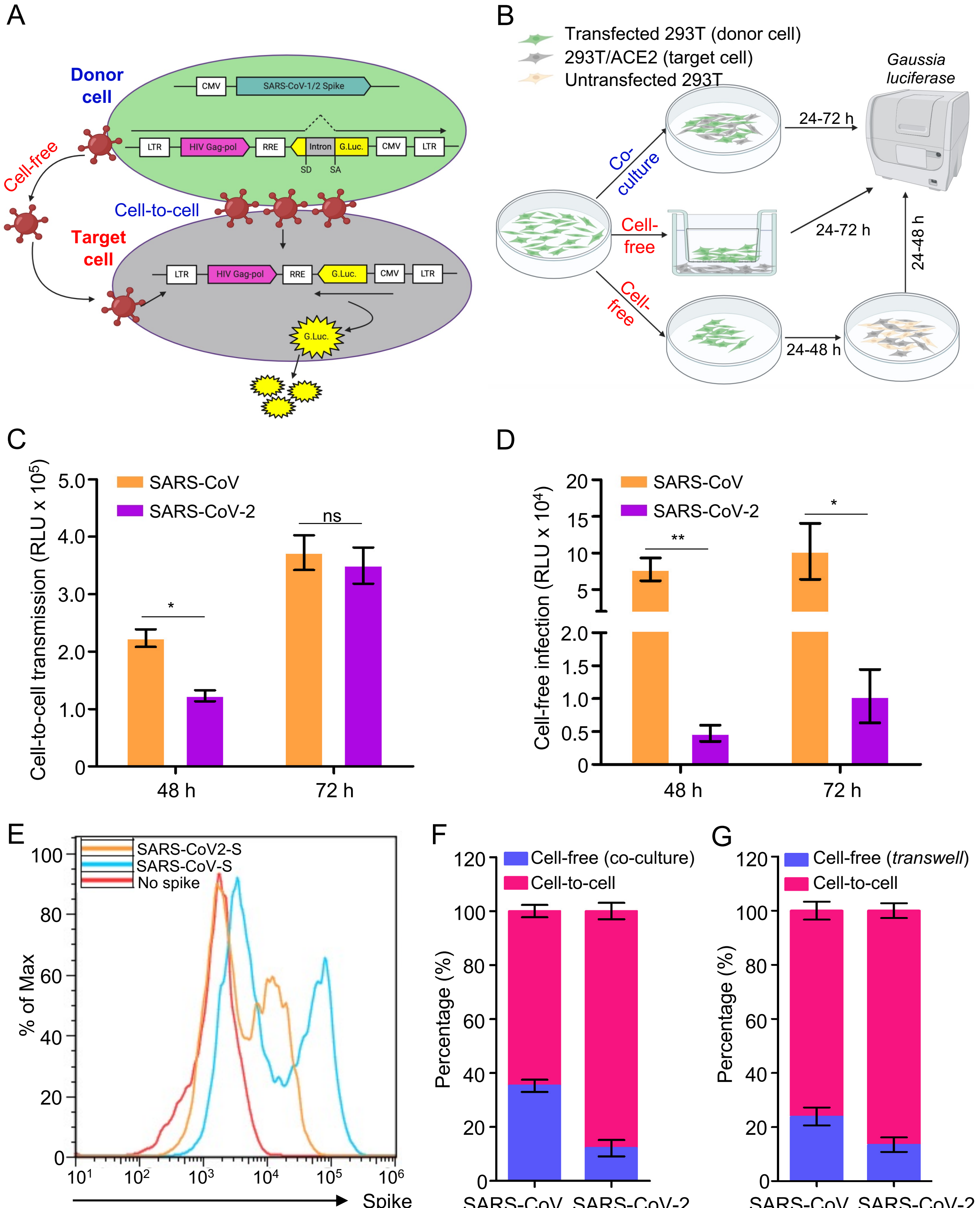

Figure 1

bioRxiv preprint doi: https://doi.org/10.1101/2021.06.01.446579; this version posted June 1, 2021. The copyright holder for this preprint (which was not certified by peer review) is the author/funder, who has granted bioRxiv a license to display the preprint in perpetuity. It is made available under aCC-BY-NC 4.0 International license.

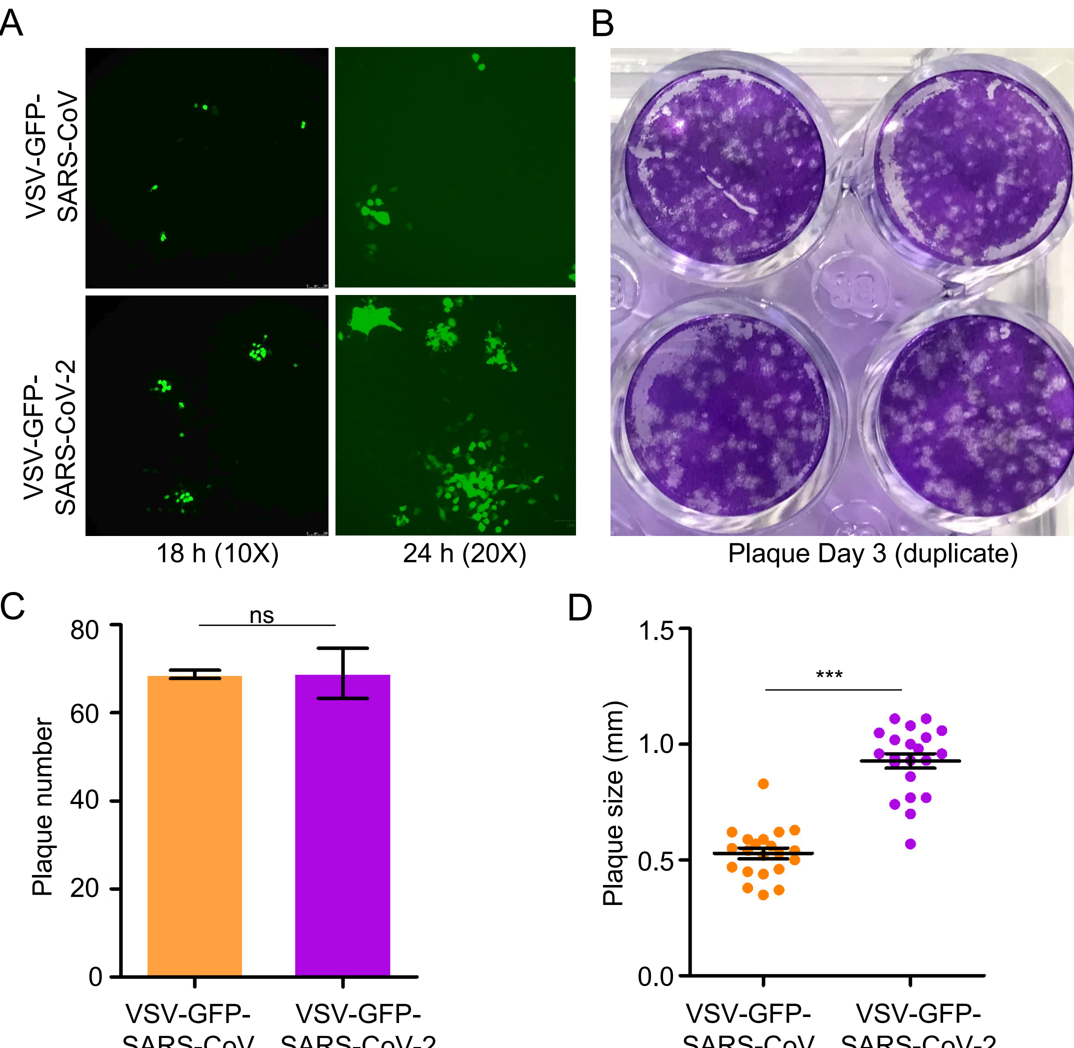

Figure 2

was not certified by peer review) is the author/funder, who has granted bioRxiv a license to display the preprint in perpetuity. It is made
available under aCC-BY-NC 4.0 International license.

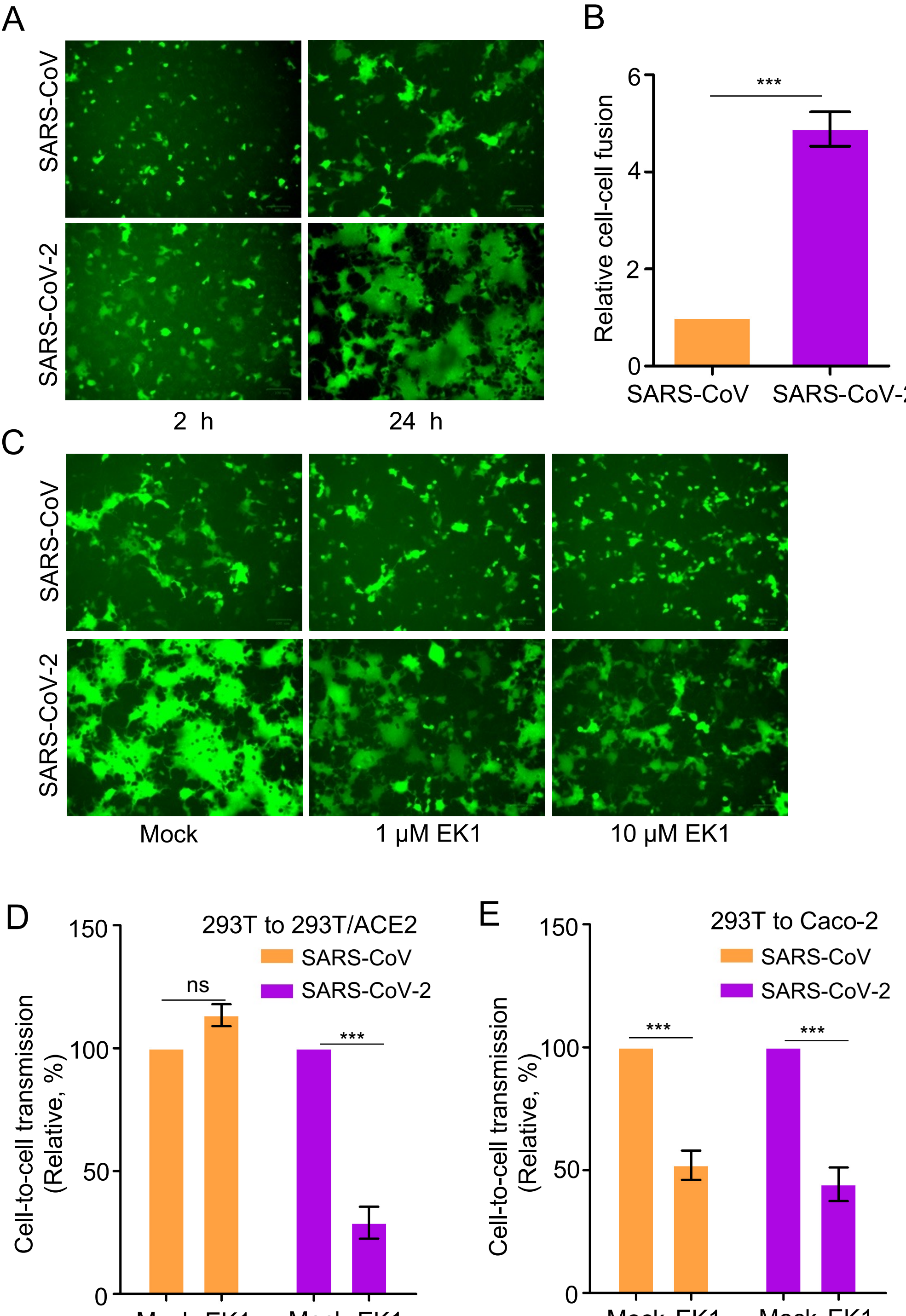

Figure 3

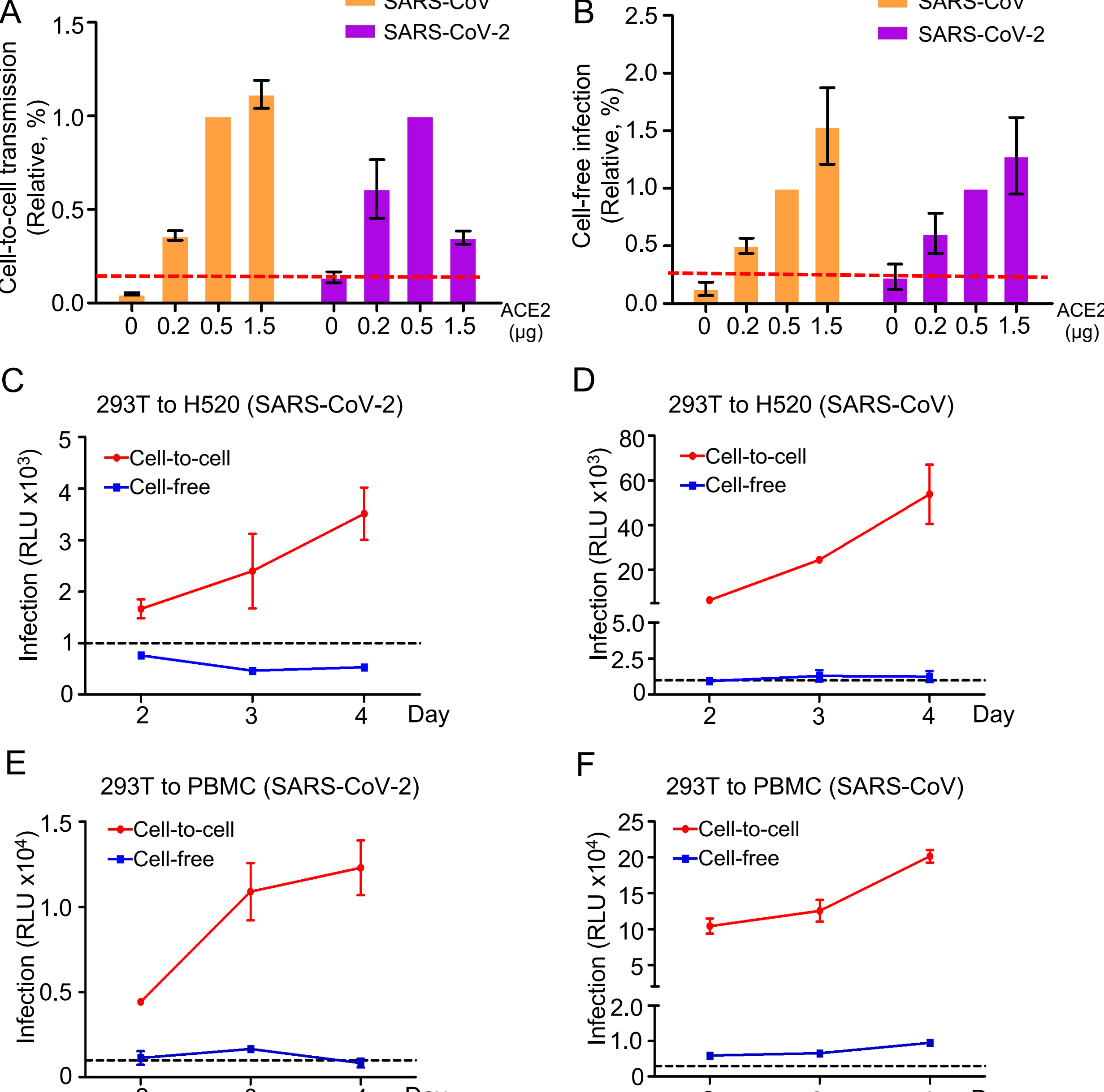

Figure 4

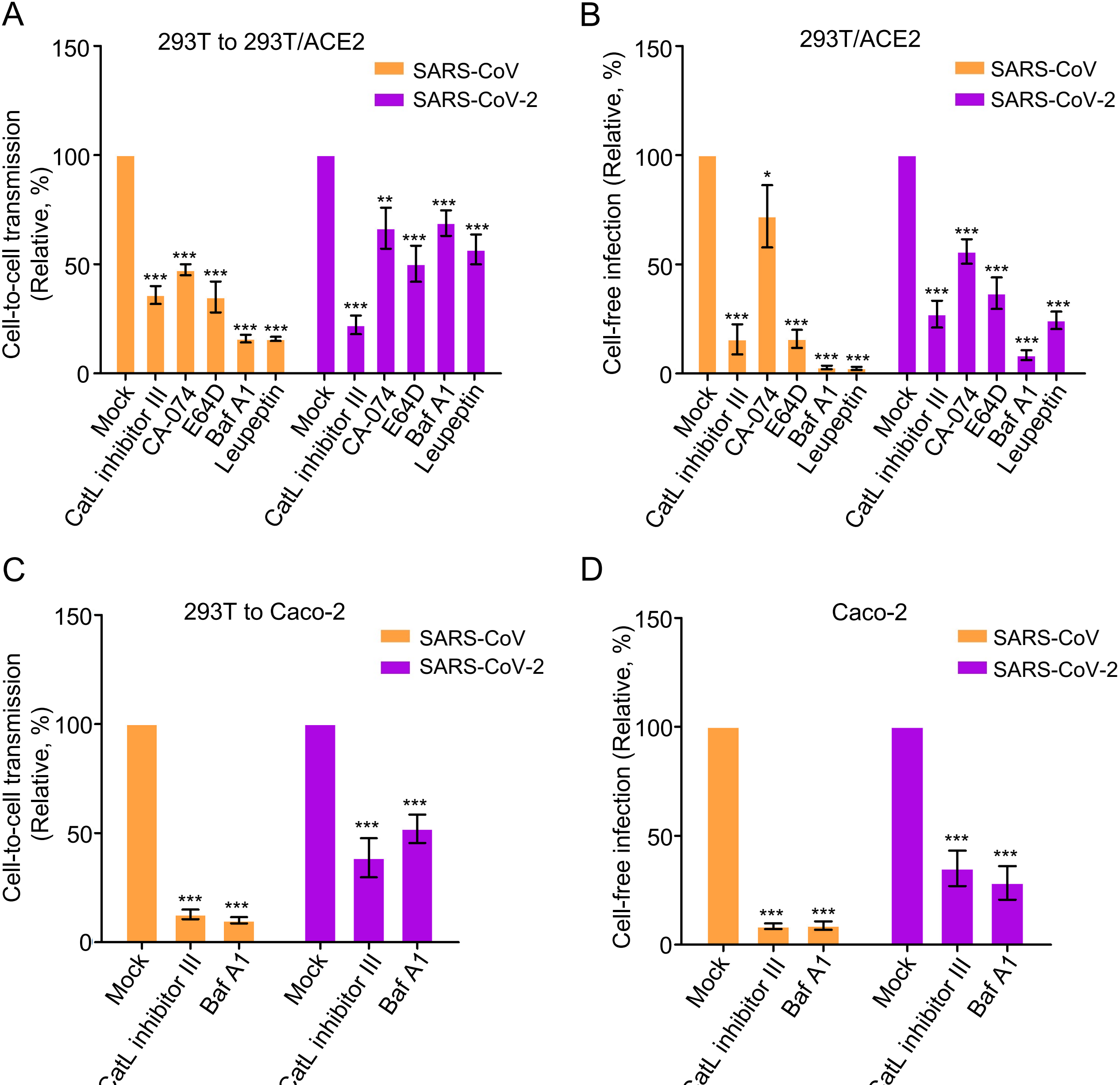

Figure 5

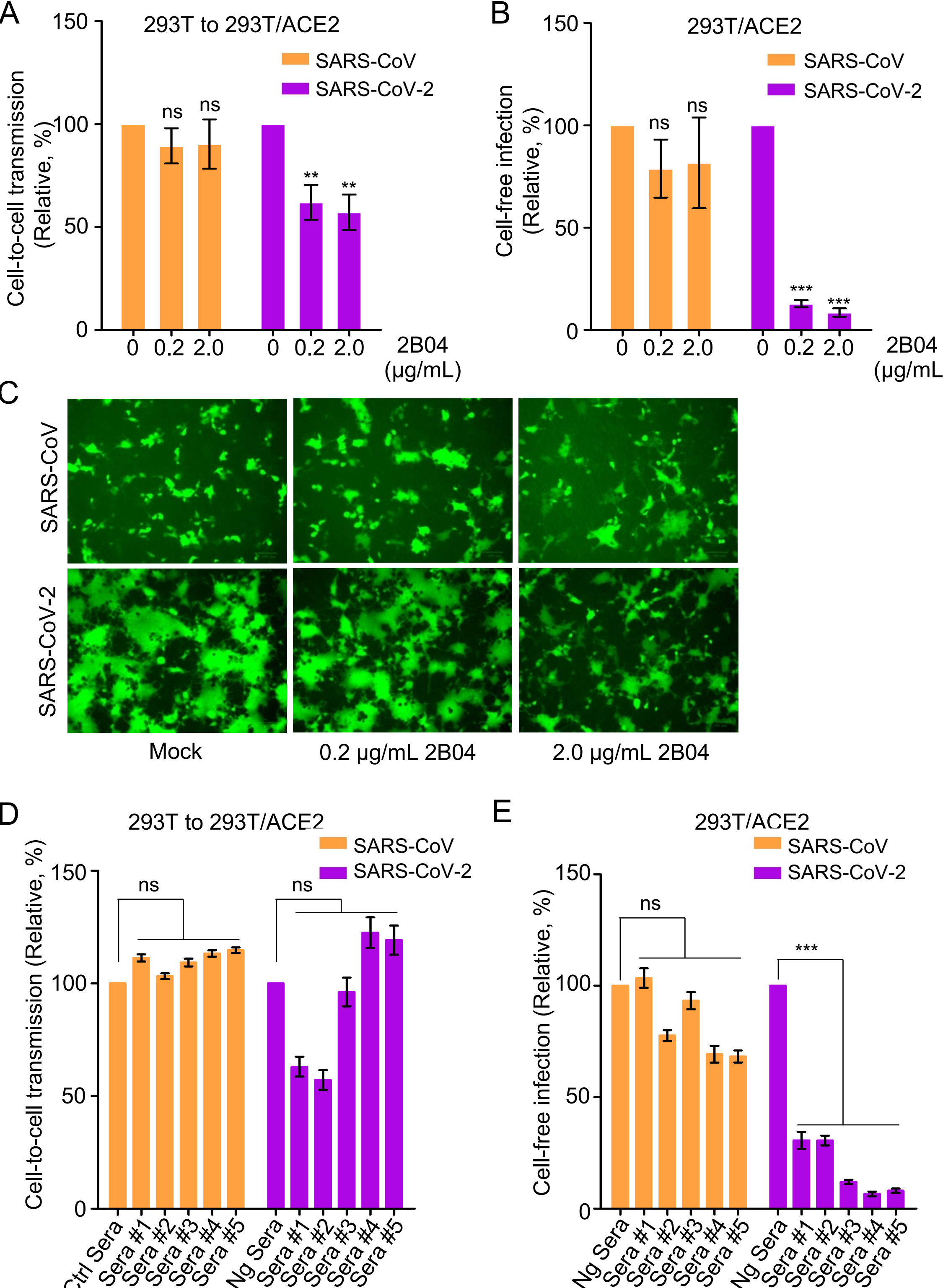

Figure 6

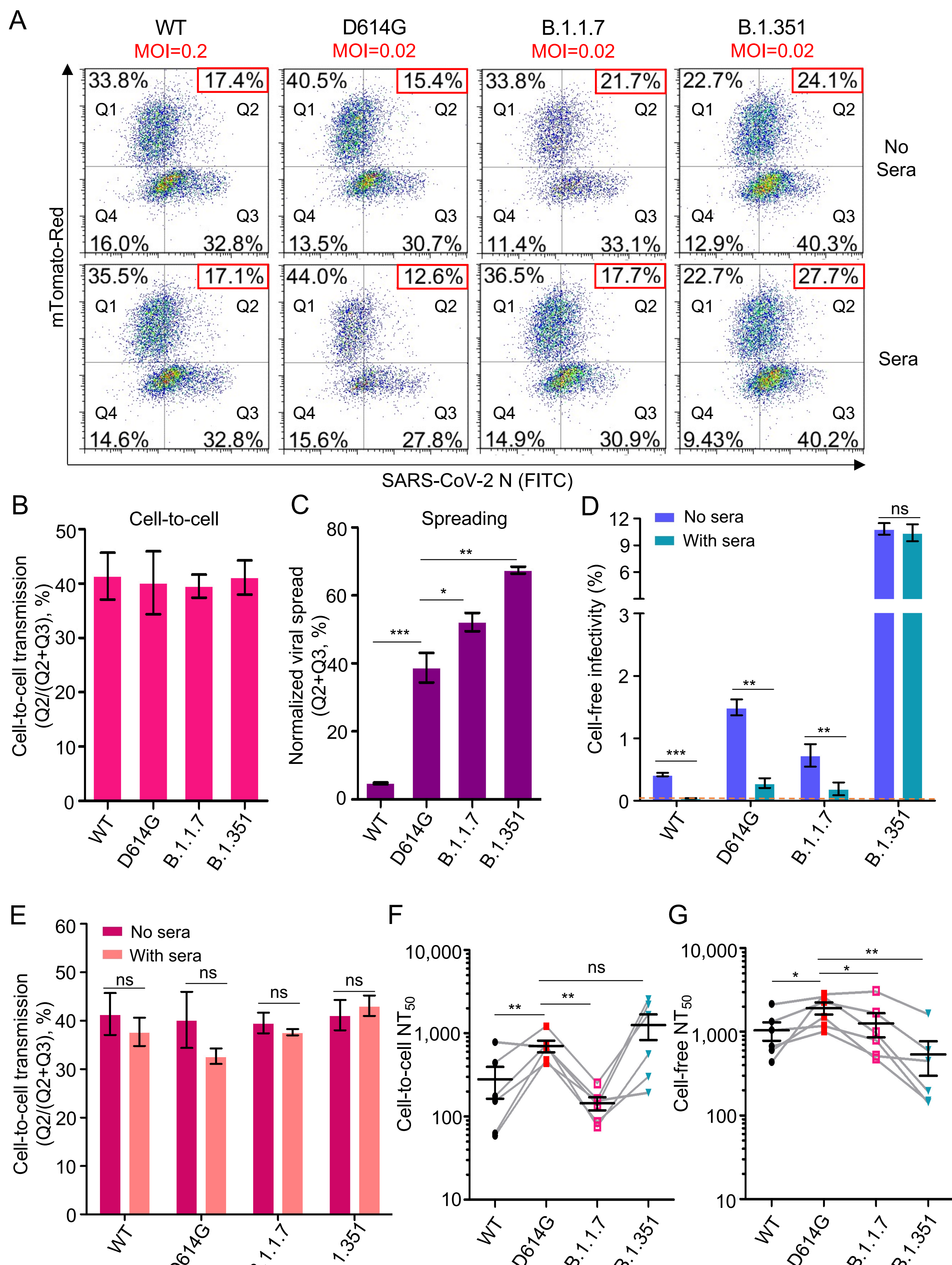

Figure 7

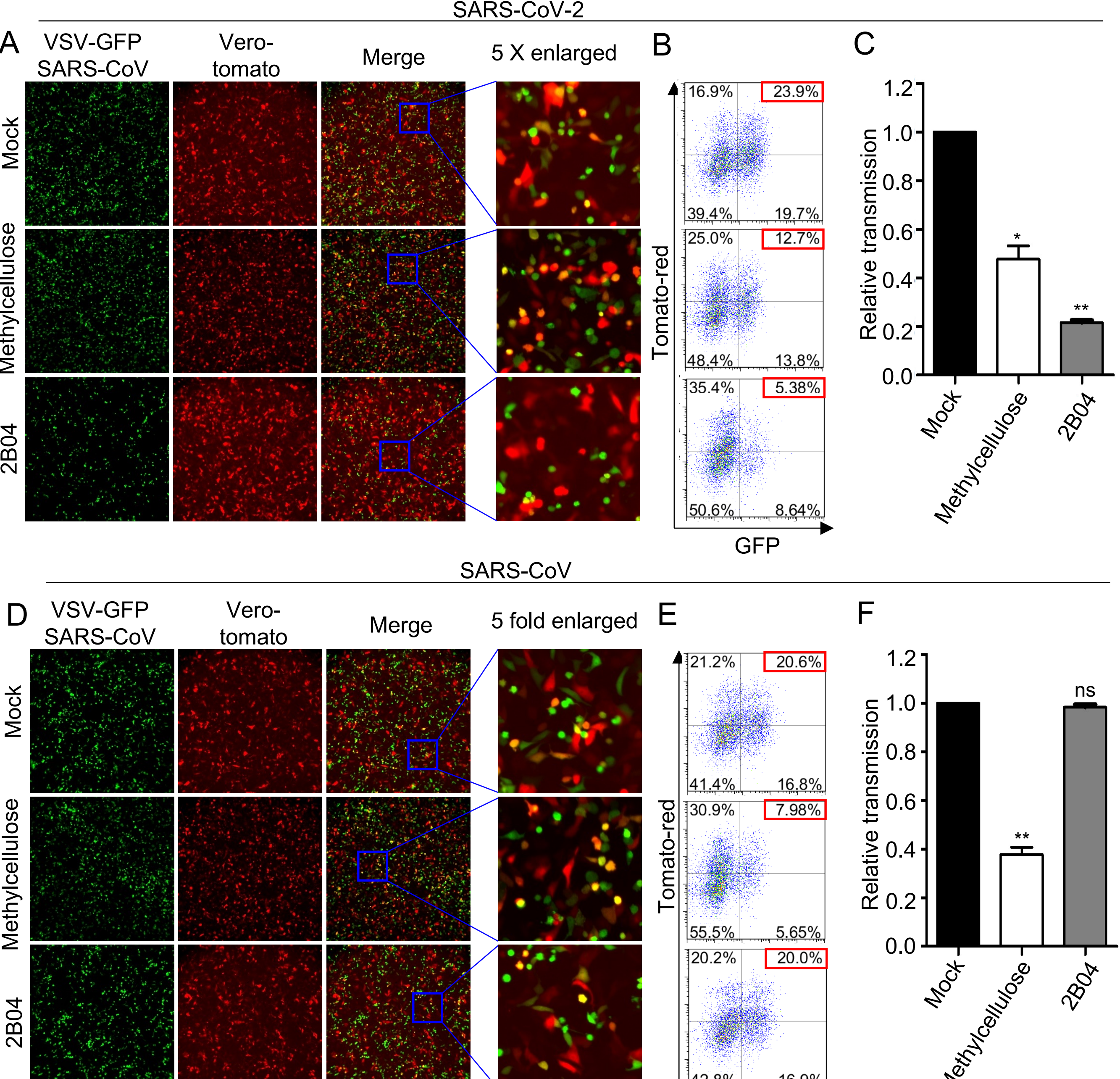

Figure S1

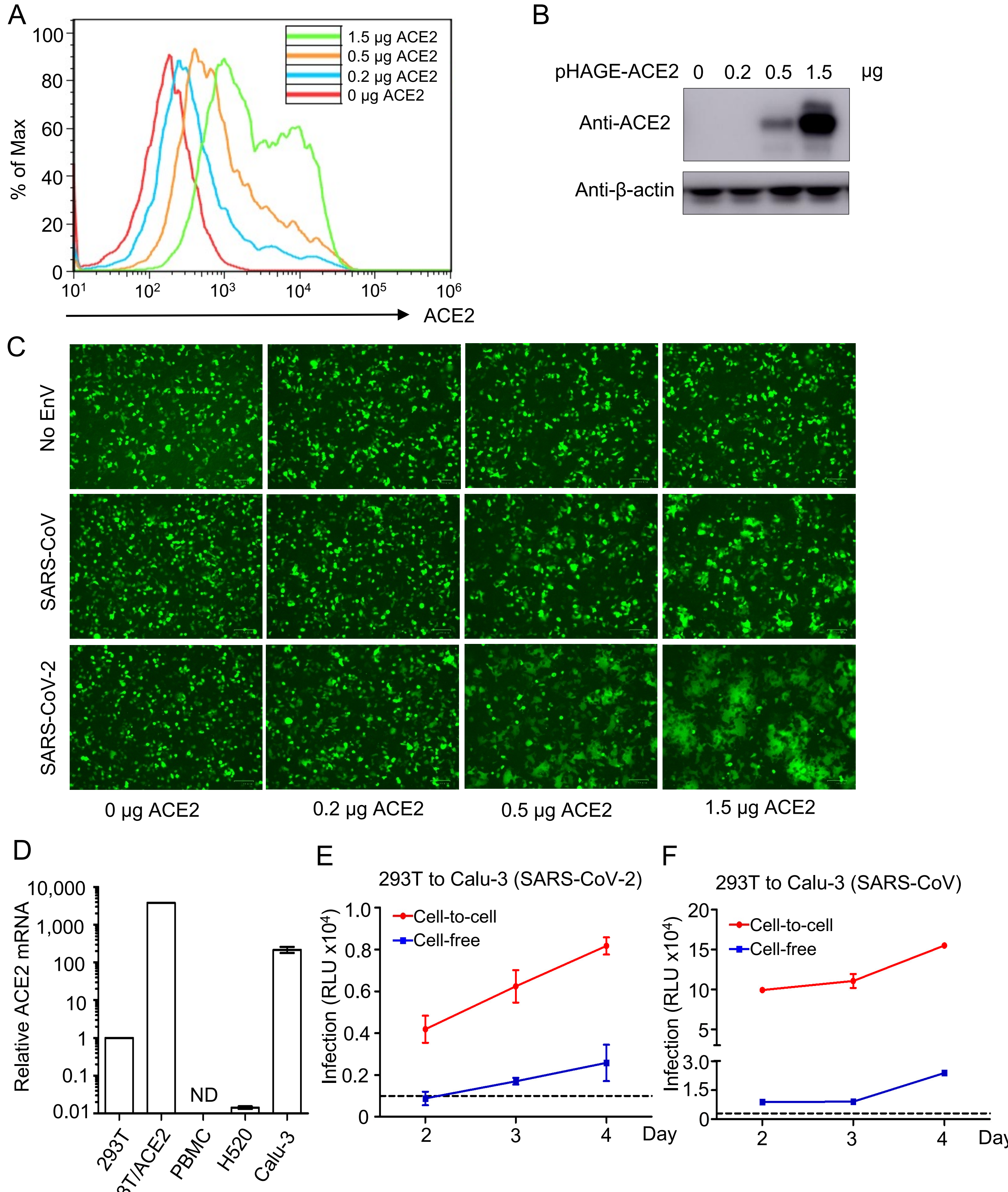

Figure S2

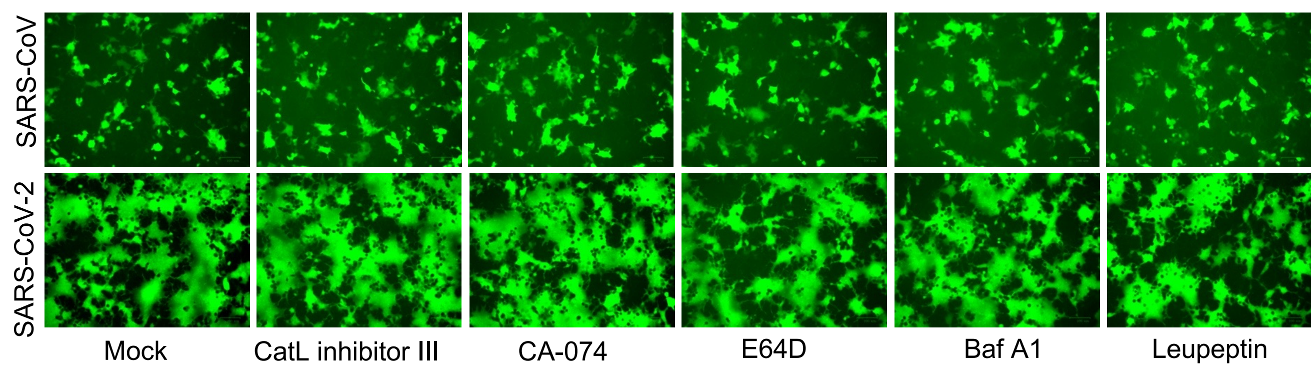

Figure S3

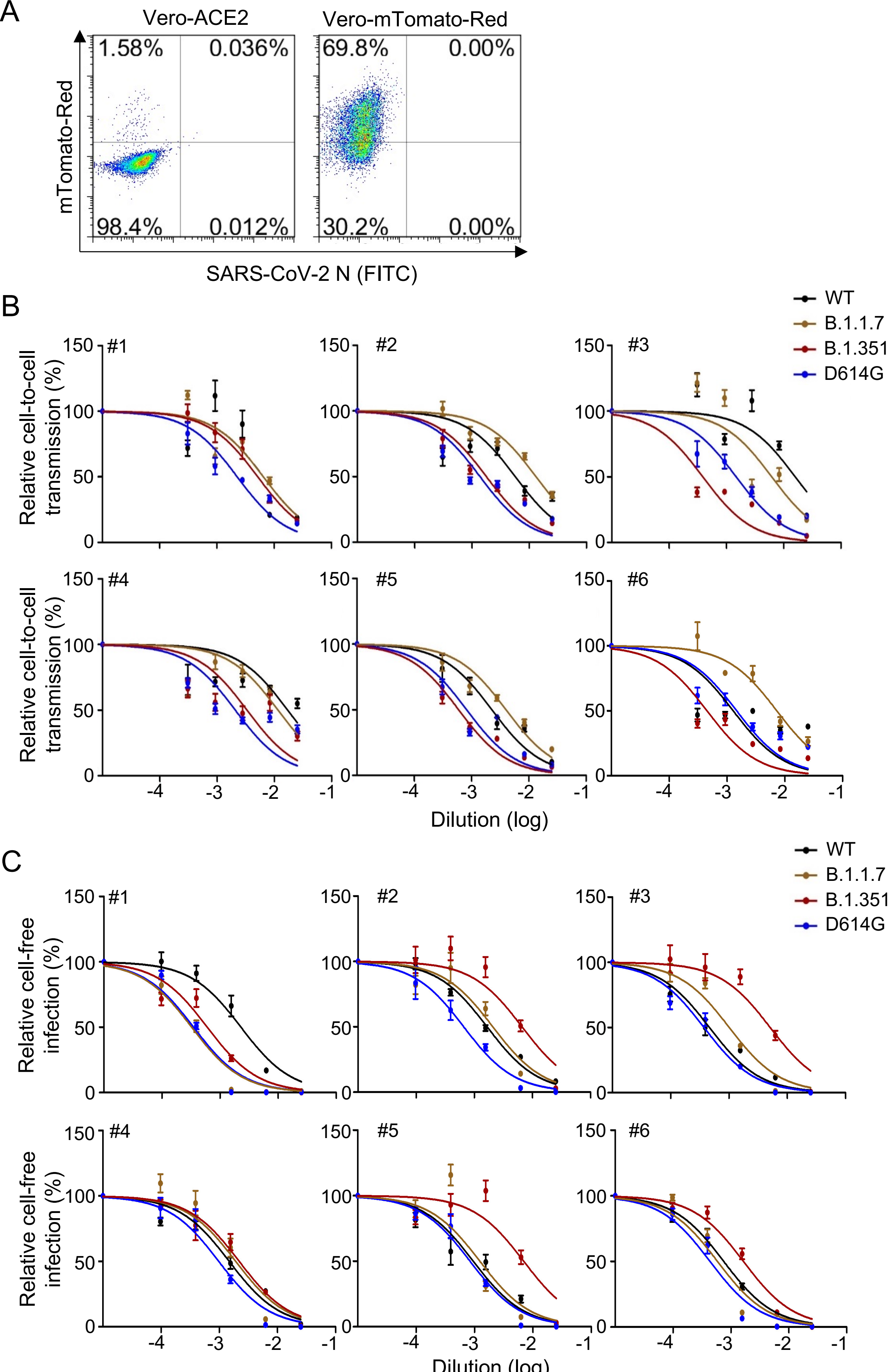

Figure S4